CULSC第十届全国大学生生命科学竞赛（创新创业类）

获奖证书

获奖项目：金属多酚网络强化冷冻保护剂对益生菌的冻干抗逆性

获奖学生：王晨 孙阿祥 王瑞 刘遥 万佳烨

指导老师：张文涛

获奖单位：西北农林科技大学

获奖类型：三等奖

证书编号：CULSC2025CS0810

全国大学生生命科学竞赛委员会

二〇二五年七月

获奖证书

蒋金霖、李鑫杰、任滋玉、谭植美、郝君艳、陶思宇、袁文轩、王晨：

你们的作品《引菇入疆——引领香菇加工新时代、产业振兴新模式》，在第九届中国国际“互联网+”大学生创新创业大赛陕西赛区省级复赛中荣获**铜奖**（高教主赛道）

指导教师：康文婧、霍海洋

特发此证，以资鼓励。

主办单位：中共陕西省委教育工委、陕西省教育厅

协办单位：中国建设银行股份有限公司陕西省分行

承办单位：西北工业大学、榆林学院

支持单位：陕西汽车控股集团有限公司

中国国际“互联网+”大学生创新创业大赛

陕西赛区组织委员会

二〇[illegible]年八月

证书编号：2023SXGJ895

Food Research International 206 (2025) 116097

Contents lists available at ScienceDirect

Food Research International

journal homepage: www.elsevier.com/locate/foodres

Metal-phenolic networks enhanced the protection of excipients for probiotics during freeze-drying

Tong Zhang [a], Chen Wang [a], Shengpeng Su [a,b], Axiang Sun [a], Ting Du [a], Jianlong Wang [a], Julong Liu [c,*], Wentao Zhang [a,*]

[a] College of Food Science and Engineering, Northwest A&F University, Shaanxi, Yangling 712100, China
[b] Inner Mongolia Enterprise Key Laboratory of Dairy Nutrition, Health & Safety, Inner Mongolia Mengniu Dairy (Group) Co., Ltd., Huhhot 011500, China
[c] Mengniu Hi-Tech Dairy Product Beijing Co., Ltd., Beijing, Tongzhou, 101107, China

ARTICLE INFO

Keywords:
Bifidobacterium bifidum
Probiotic powder
Freeze-drying
Nanoencapsulation

ABSTRACT

Probiotic powder using a single protective method during freeze-drying is insufficient vitality because it lacks adequate protection. Here we developed a protection strategy through biointerfacial phenolic self-assembly to enhance the protection of excipients for probiotics to address existing challenges during freeze-drying. This strategy could strengthen the connections of excipients and phenolic protective layers containing hydroxyl groups with water molecules, improving the hydration layer's preservation and shielding bacteria from damage. The results indicated that, compared with origin probiotics, protected probiotics maintained higher viability at approximately 91 % and higher ATPase activity and exhibited a better survival rate in various environmental challenges after freeze-drying. The broad applicability of this protection strategy was confirmed across other LAB strains. Additionally, the protected probiotics demonstrated superior shelf life during 30 days of storage, indicating promising prospects for preparing bacterial powder via freeze-drying.

1. Introduction

Probiotics, defined as live microorganisms that provide a health benefit to the host when administered in adequate amounts, are widely applied in the fermented food industry and health care products, deepening consumers' affection and faith due to their functional properties including disease prevention, immunity enhancement, and modulating intestinal microbial balance (Fenster et al., 2019; George Kerry et al., 2018; Kechagia et al., 2013). Currently, dried probiotic products have been commercialized, and their market is rapidly expanding (Yuan et al., 2022). However, their health benefits have been shown that hosts need to use live probiotic cells, not probiotic products (Kothari et al., 2019). Probiotics suffer from many challenges including the processing conditions and harsh gastrointestinal tract. Maintaining high probiotic activity during production and oral consumption is crucial.

Freeze-drying, which directly converts free water inside and outside the cell into gas, is gradually gaining acceptance as it effectively prevents deterioration caused by microbial activity and protein denaturation (Tian et al., 2024), but the formation of ice crystals at the freezing stage can damage the structure and function of probiotics at drying process to induce cellular stress and decrease viability (Ge et al., 2024). The addition of cryoprotectants is often used to tackle the problem of insufficient probiotic activity in freeze-drying. Therefore, various types of cryoprotectants, such as trehalose, skim milk, and sucrose, have been investigated to meet the demands of efficient production. Despite the interest and significant development of cryoprotectants in recent decades, single cryoprotectants are still unable to retain the high probiotic activity in freeze-drying and their efficacy is strain-dependent (Fan et al., 2022; L. Liu et al., 2024). Metal-phenolic networks form on a variety of substrates through nucleation and subsequent self-assembly (Du et al., 2023; Du et al., 2024; Shi et al., 2024). Fe^{3+}- Tannic acid (TA) films (MPN) have been shown to readily form on numerous biotic surfaces, including eukaryotes, yeast, and microbes (Xie et al., 2021). Currently, Fan et al. (2022) have applied Fe^{3+}-TA films in *Escherichia coli Nissle* 1917 to resist processing stressors of freeze-drying, which has proven that this self-assembling coating can improve the viability and stability of anaerobic microbes. Additionally, MPN-coated microbes have shown a higher survival rate after freeze-drying even in the absence of conventional cryoprotectants. Other studies also showed the

* Corresponding authors.
E-mail addresses: liujulong@mengniu.cn (J. Liu), zhangwt@nwsuaf.edu.cn (W. Zhang).

https://doi.org/10.1016/j.foodres.2025.116097
Received 16 October 2024; Received in revised form 9 February 2025; Accepted 22 February 2025
Available online 24 February 2025

protection of MPN for probiotics in environmental assaults. For example, probiotics coated with tannic acid and mucin (EcN@TA-Ca^{2+}@Mucin) exhibited superior resistance, strong adhesiveness, and distinctly down-regulate inflammation with ROS scavenging (X. Yang et al., 2022). The double-layer coating strategy encapsulates probiotics in a TA/Fe (III) MPN (interior layer) and enteric L100 layers, which could protect probiotics against the acidic environment (J. Liu et al., 2021). However, the protection of MPN for anaerobic microbes has not been determined during freeze-drying whether it meets the industry requirement for the number of viable bacteria. The protective capabilities of current single agents vary widely among probiotics and are insufficient, necessitating the development of more advanced and effective multiple protection strategies.

In response to these demands, a protected method was designed in this study using biointerfacial phenolic self-assembly to enhance the protection of excipients for probiotics, aiming to help probiotics maintain vitality during freeze-drying, with *Bifidobacterium bifidum* (B.B.) representing probiotics and trehalose representing excipients. The formation of MPN on the surface of B.B. was first characterized. Then, after freeze-drying, the optimum protected concentration of MPN and trehalose for B.B. was determined. Furthermore, the effects of the dual-protected method for B.B., including the survival rate and ATPase activity, were systematically investigated. At last, the broad applicability of the dual-protected method in other LAB strains and the storage stability were determined. Thus, a new approach was used to prepare probiotic powder with long-term stability after freeze-drying, facilitating the development of probiotic strains of interest by ensuring their post-production viability.

2. Materials and method

2.1. Materials

All LAB strain was acquired from the Northwest A&F University (Yangling, Shaanxi). Tannic acid and $FeCl_3$ were purchased from Shanghai Aladdin Biochemical Technology Co., Ltd. (Shanghai, China). Trehalose was purchased from Shanghai Yuanye Co. Ltd. (Shanghai China).

2.2. The formation of MPN on the surface of B.B.

At first, to determine the effect of TA and Fe^{3+} on B.B., we evaluate the living cells for B.B. at different concentrations of TA (0.4, 0.8, 1.2, 1.6 mg/mL) and Fe^{3+} (0.06, 0.12, 0.18, 0.24 mg/mL). The aqueous suspension of B.B. (100 μL) was inoculated with MRS culture medium (5 mL) containing different concentrations of TA and Fe^{3+}, respectively, and then incubated at 37 °C for 10 h in anaerobiosis to ensure the optimum concentration of TA and Fe^{3+}.

Then, the formation of MPN on the surface of B.B. was according to Fan et al. (2022) with slight modifications. The optimum concentration of TA (250 μL) and $FeCl_3$ (250 μL) were added sequentially to the aqueous suspension of B.B. (500 μL,10^8 CFU/mL), and then the solution was mixed vigorously for 10 s. The MOPS buffer (1 mL, 20 mM, pH 8) was added to the mixture for the formation of a stable MPN shell.

2.3. Characterization analysis

Scanning electron microscopy (SEM, S-4800, Hitachi) was applied to detect the surface of probiotics. The preparation of samples was as follows. Briefly, glass coverslips were initially placed in the probiotic solution and kept at 4 °C for 30 min. After removing the unattached probiotics, the cells were fixed with glutaraldehyde (2.5 %) for 6 h at 4 °C. Subsequently, a serial ethanol dehydration process with 30 %, 50 %, 70 %, 90 %, and 100 % was implemented. Finally, the samples were dried using CO_2 critical point drying. FTIR spectrometer (Vertex70, BRUKER Corp, Germany) was used for analyzing the intermolecular interactions between B.B. and MPN and measured according to L. Liu et al. (2024). Briefly, different samples were mixed with KBr (1:100) to make transparent tableting, and then the transparent tableting was directly used for FTIR spectroscopy. UV–Vis Spectrophotometer (MAPADA P7, China) was used to confirm the formation of MPN.

2.4. Preparation of the LAB powder

Firstly, different probiotic samples were washed with sterile water three times, and precipitation was added to the different concentrations of trehalose at the last time. Samples were stored at −80 °C for 12 h and then immediately lyophilized for 12 h, with a cold trap temperature of −80 °C and a vacuum degree of 3.5 Pa. During all freeze periods, the samples should be kept from melting. After freeze-drying, the agents were sealed immediately and stored at −20 °C.

2.5. Determinations of cell viability and activity

2.5.1. Survival rate

Standard plate counting was applied to measure the growth of LAB strains. Different treatments before and after freeze-drying were prepared to count, and the plates were incubated at 37 °C for 48 h anaerobically. The survival rate was calculated using the following eq. (1):

$$\text{Survival rate}\ (\%) = \frac{B_1}{B_0} \tag{1}$$

where B_0 is the living cells before freeze-drying and B_1 is the living cells after freeze-drying.

2.5.2. Determination of ATPase activity

We selected two types of ATPase activity, including Na^+-K^+-ATPase activity and Ca^{2+}-Mg^{2+}-ATPase, in order to determine the activity of probiotic powers. All samples were analyzed using an activity assay kit (BOXBIO, Beijing, China). ATPase is capable of decomposing ATP into ADP and phosphorus. The ATPase activity was determined by analyzing the absorbance value of phosphorus at 660 nm, with a 0.5 μmol/mL phosphorus solution serving as the standard. ATPase activity was calculated through Eqs. (2), (3).

$$Na^+ - K^+ - \text{ATPase activity}\ (U) = \frac{OD_M - OD_c}{OD_{SD} - OD_B} \times 7.5 \times C_{total} \tag{2}$$

$$Ca^{2+} - Mg^{2+} - \text{ATPase activity}\ (U) = \frac{OD_M - OD_c}{OD_{SD} - OD_B} \times 7.5 \times C_{total} \tag{3}$$

where OD_M stands for the absorbance value of the sample, OD_C is the absorbance value of the control, OD_{SD} is the absorbance value of the standard solution, OD_B represents the absorbance value of the blank, and C_{total} represents the count of bacteria.

2.6. The storage stability

To provide a comprehensive understanding of the storage stability of the probiotic powders under different temperature conditions, freeze-dried samples (10 mL) were divided into equal parts and stored in the dark at 4 °C and − 20 °C for 30 days. The living cells were periodically measured every three days through the plate counting method.

2.7. Statistical analysis

The data were presented as the mean ± standard deviation (SD), with all experiments conducted in triplicate. Statistical analysis was performed using ANOVA with IBM SPSS 22 software, and significant differences ($P < 0.05$) were determined by Duncan's test for significant differences.

3. Results and discussion

3.1. The formation of MPN on the surface of B.B.

We first analyzed the effect of MPN, TA, and Fe^{3+} for B.B. to determine the optimum concentration of MPN formation. As shown in Fig. 1a, B.B. maintained the higher activity at the concentration of MPN formation at 0.8 mg/mL TA and 0.12 mg/mL Fe^{3+} than other concentrations. The activity of B.B. was slightly inhibited due to existing TA (Fig. S1), but B.B. maintained a higher activity than the different concentrations of Fe^{3+}. Although living bacteria counts were decreased with the increase of Fe^{3+}, we chose the relatively higher 0.12 mg/mL Fe^{3+} to ensure the protection of MPN due to no significant difference at 0.12 mg/mL and 0.06 mg/mL (Fig. S2). According to Fan et al. (2022), the concentration of TA was determined to be 0.8 mg/mL due to no significant difference among different concentrations of TA. Therefore, 0.8 mg/mL TA and 0.12 mg/mL Fe^{3+} were verified at the optimum concentration of the formation of the MPN. We then verified the formation of MPN on the surface of B.B. (B.B.@MPN) by UV–vis spectra, FTIR spectral analysis and SEM. Notably, a significantly sharper peak at around 1450 cm^{-1} and 1365 cm^{-1} (Fig. 1d), representing methyl (–CH3) group, got stronger from the B.B.@MPN group to the control group (B.B.). The peak intensity at 1061 cm^{-1} for the B.B.@MPN group can be attributed to the stretching vibration of C—O (Luo et al., 2022; Zhang et al., 2019). Meanwhile, the B.B.@MPN group found a new peak in the regions between 3500 and 3100 cm^{-1} with peaks at 3300 cm^{-1}, which were dominated by bands assigned to the intermolecular hydrogen bonding (Martins et al., 2023). In UV–vis spectra (Fig. 1d), compared with B.B., the B.B.@MPN group had appeared peak shift and new peak between 210 and 350 nm. SEM images confirmed MPN assembly, showing individual B.B. encapsulated in Fe^{3+}–TA complexes, as indicated by their small surface particles (Fig. 1c (ii) and (iii)), while the surface of uncoated B.B. was smooth (Fig. 1c (i)). The results further confirmed that the MPN forms on the surface of probiotics.

3.2. The protection of trehalose with MPN for B.B. In freeze-drying

Freeze-drying is often used in the drying of probiotics, but as few as 0.1 % of cells survive, which is woefully inadequate for daily use (Fan et al., 2022). This work evaluated the dual protection effect including nanoencapsulation and adding excipients for B.B. in freeze-drying to improve probiotic cells survive. Fig. 2a shows the effect of freeze-drying on the viability of all treatments. The survival rate of trehalose (10 mg/mL) with MPN for B.B. (trehalose with MPN@B.B.) reached 31.43 ± 0.78 %, while the B.B. and B.B.@MPN only had 1.45 ± 0.06 % and 10.61 ± 1.06 % of cells survived, which showed the limited protective effect of nanoencapsulation. To improve the survival rate for unprotected cells, we tried to increase trehalose concentration. As shown in Fig. 2b, when the concentration of trehalose was increased to 30 mg/mL, the survival rate of protected cells increased to more than 90 %, and a further increase in trehalose concentration did not significantly increase cell survival. The survival rate for single trehalose with unprotected cells only reached 59.20 ± 5.23 % as the trehalose concentration had reached 120 mg/mL, and increasing the trehalose concentration did not significantly improve the survival of the cells (Fig. 2c). Trehalose molecules can entrap bulks of water to form the hydration layer and react with the water molecules forming hydrogen bonds to stabilize the protected molecule against damage (Siri et al., 2016). L. Liu et al. (2024) proved that 1 % sodium carboxymethyl cellulose had better protective effects compared with other cryoprotectants in 5 % concentration, and sodium carboxymethyl cellulose-treated probiotics only held a survival rate of 22.44 ± 2.21 %, while in our work, the survival rate of B.B. protected by 10 mg/mL trehalose and MPN had reached 30 %. Therefore, the synergistic protection of probiotic cells using nanoencapsulation and trehalose may be due to the enhancement of hydrogen bonds between trehalose and MPN during freeze-drying. Then, we measured the FTIR spectra of all treatments after freeze-drying to prove the formation of hydrogen bonds at water molecules, trehalose, and MPN. As shown in Fig. 2d, the broad band between 3000 cm^{-1} and 3600 cm^{-1} was mainly attributed to O—H stretching from absorbed water (Singh et al., 2017). The characteristic peaks in the B.B. and B.B.@MPN at 3290 cm^{-1} and

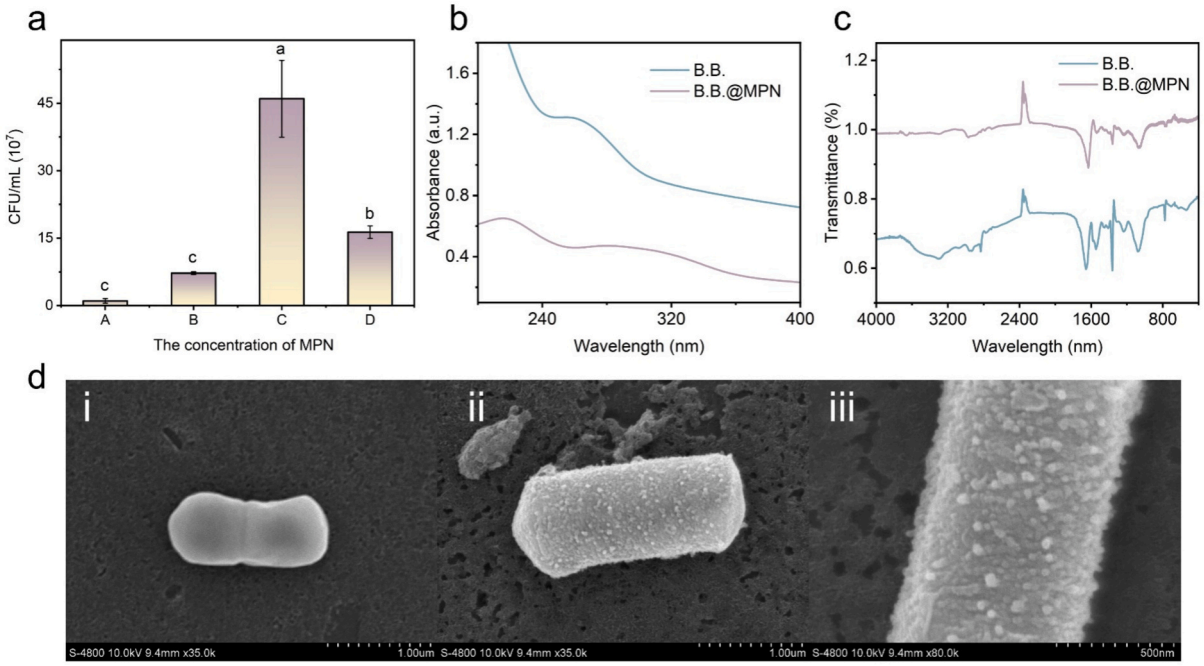

Fig. 1. Characterization of the formation of MPN on the surface of probiotics. Effect of the concentration of MPN for B.B. (A: 0.16 mg/mL TA and 0.24 mg/mL Fe^{3+}, B: 1.2 mg/mL TA and 0.18 mg/mL Fe^{3+}, C: 0.8 mg/mL TA and 0.12 mg/mL Fe^{3+}, D: 0.4 mg/mL TA and 0.06 mg/mL Fe^{3+}). UV–vis spectra (b) and FTIR spectra (c) of B.B. and B.B.@MPN. SEM images (d) of B.B. and B.B.@MPN (i: B.B., ii: B.B.@MPN, iii: local enlarged B.B.@MPN). Significant differences according to Duncan's test ($P < 0.05$) among samples are represented by different lowercase letters.

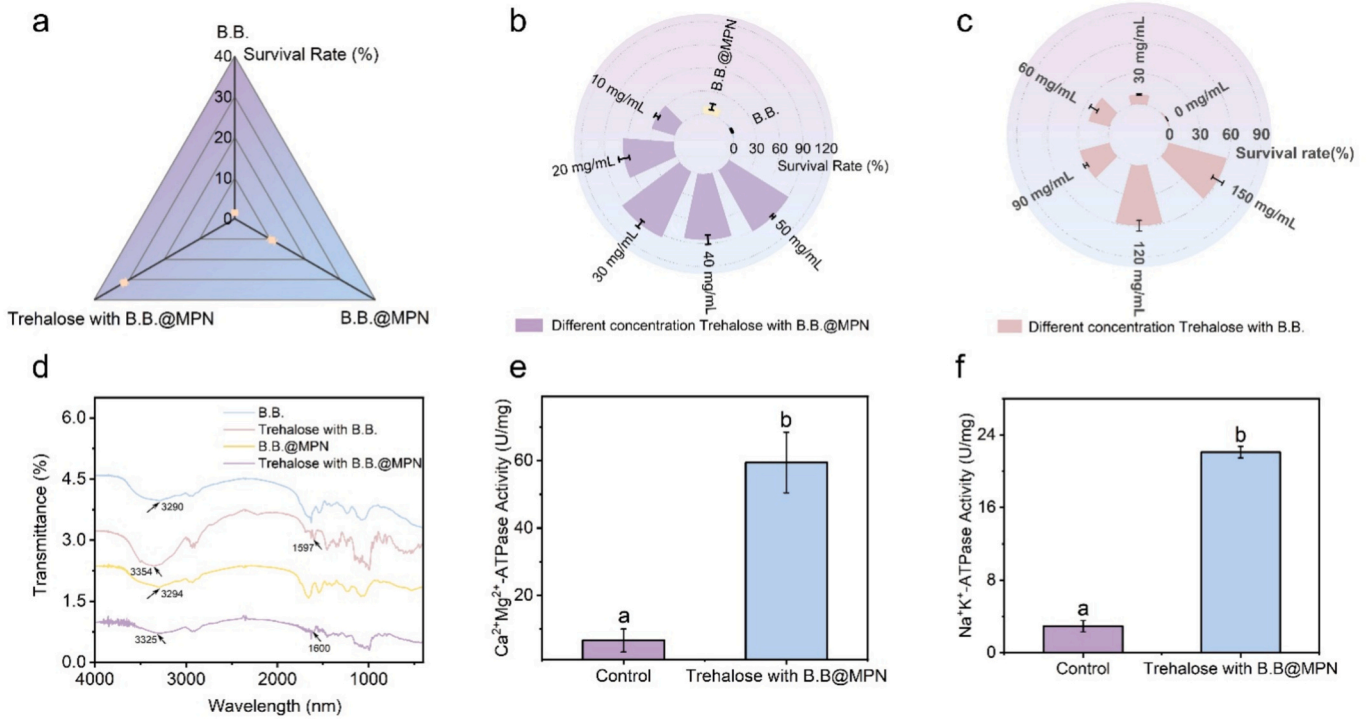

Fig. 2. The protection of trehalose with MPN for B.B. in freeze-drying. (a) The survival rate of different treatments in freeze-drying and the concentration of trehalose of 10 mg/mL. The effect of different concentrations of trehalose on the survival rate of B.B.@MPN (b) and B.B. (c) in freeze-drying. (d) FTIR spectra of different treatments after freeze-drying. (e) Ca^{2+}-Mg^{2+}-ATPase activity and (f) Na^{+}-K^{+}-ATPase activity of B.B. and B.B.@MPN. Significant differences according to Duncan's test ($P < 0.05$) among samples are represented by different lowercase letters.

3294 cm^{-1} were attributed to the O—H stretching band of the hydroxyl groups (Deng et al., 2021; Li et al., 2020), while these absorption peaks exhibited a shift in the trehalose with B.B. (3354 cm^{-1}) and trehalose with B.B.@MPN (3325 cm^{-1}) due to the effect of the hydrogen bond (Martins et al., 2023). Meanwhile, trehalose with B.B. and trehalose with B.B.@MPN appeared to have new characteristic peaks at 1597 cm^{-1} and 1600 cm^{-1}. The FTIR spectra of trehalose with B.B. were similar to those of single trehalose (Fig. S3), whereas the spectra of trehalose with B.B.@MPN differed from those of single trehalose. This occurred as trehalose and MPN layers containing hydroxyl groups created connections with water molecules, which attached to free water in the system and interacted with the ice interface through hydrogen bonding, hydrophobic interactions, or electrostatic interactions. These connections prevented the formation of ice crystals, thus improving the

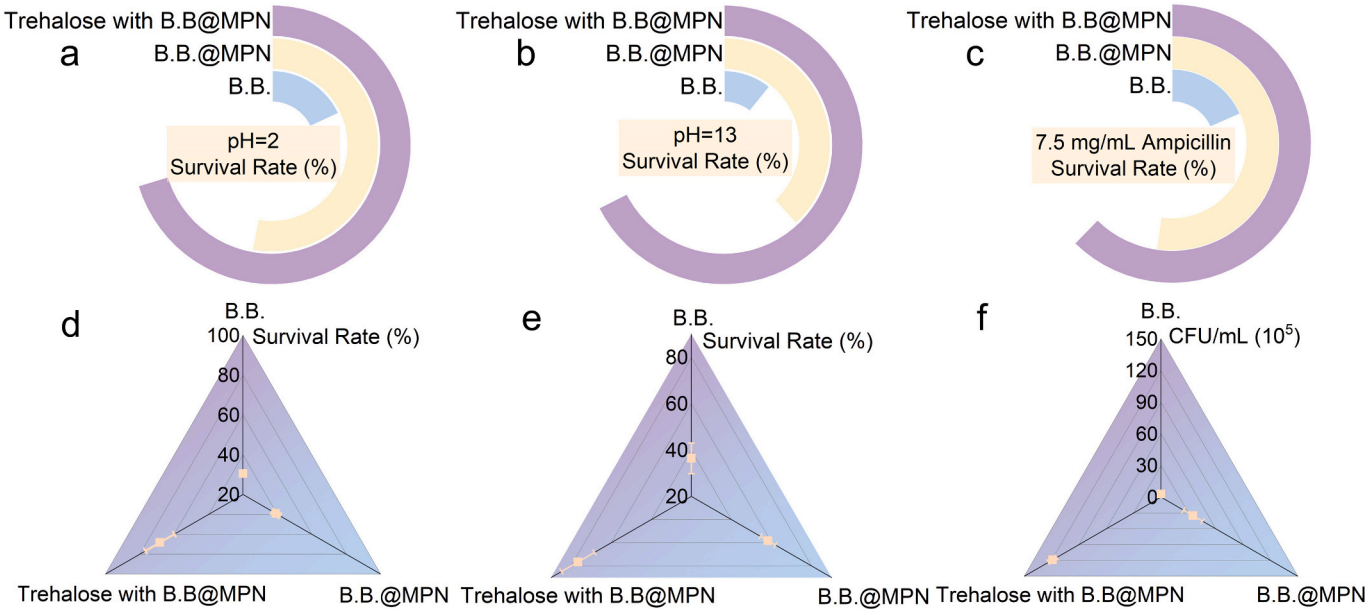

Fig. 3. The vitality of probiotic powders after freeze-drying in environmental assaults. Survival rate of different treatments at (a) pH = 2, (b) pH = 11, (c) 7.5 mg/mL ampicillin, (d) SGF (pH 1.2), (e) SIF (pH 6.8) at 37 °C, and (f) 0.3 mg/mL bile salts. Significant differences according to Duncan's test ($P < 0.05$) among samples are represented by different lowercase letters.

preservation of the hydration layer and shielding bacteria from damage caused by mechanical and osmotic stress from ice crystals (Jia et al., 2022; Novak & Grdadolnik, 2021; Zhao et al., 2024). Fig. 2e and f show that there is a significant difference in ATPase activity between B.B. and trehalose with MPN@B.B., further indicating that MPN enhanced the protection of excipients for probiotics.

3.3. The survival rate for environmental assaults

The probiotic power must demonstrate safety and efficacy in humans, while maintaining viability throughout the product's shelf life (Williams, 2010). We then examined the survival and growth of various probiotic powers after Freeze-drying in the presence of multiple environmental stressors, including antibiotics, strong acidity, and alkalinity, as well as intestinal conditions such as acidic pH, enzymes, and bile salts. In strong acidity and alkalinity (Fig. 3a and b), trehalose with MPN@B.B. showed a higher survival rate than other treatments, similar to the results observed with antibiotics (Fig. 3c). Then, we evaluated the vitality of probiotic powder in simulated gastroenteric environments including simulated gastric fluid (SGF) with added pepsin (pH 1.2), simulated intestinal fluid (SIF) containing trypsin (pH 6.8) and bile salts (0.3 mg/mL) (Fig. 3d-e). Trehalose with MPN@B.B. consistently maintained superior vitality compared to other treatments. In SGF, the survival rate of B.B. was only 30.49 ± 1.17 %, whereas trehalose with MPN@B.B. demonstrated a significantly higher survival rate of 68.31 ± 8.42 % (Fig. 3d). This same trend was observed in SIF as well (Fig. 3f). The vitality of trehalose with MPN@B.B. in bile salts was 40 times higher than that of B.B., and 3 times higher than that of B.B.@MPN. Therefore, it was evident that the synergistic effect of trehalose and MPN provided excellent protection for probiotics.

3.4. The protective effect on other LAB strains

To demonstrate the broad applicability of adding trehalose to MPN-protected probiotics as a co-protection strategy in freeze-drying, 5 LAB strains other than Lb. *Bifidobacterium bifidum*, including *Lactobacillus plantarum* (L.p.), *Lactobacillus acidophilus* (L.a.), *Lactobacillus brevis* (L.b.), *Lactobacillus casei* (L.c.), *Lactobacillus paracasei* (L.pc.), were tested for their survival rate, Na^+-K^+-ATPase, and Ca^{2+}-Mg^{2+}-ATPase activity. Overall, adding trehalose to MPN-protected probiotics significantly increased viability compared to the unprotected group, although the protective effect varied among different LAB strains. Survival rates in Fig. 4a showed that L.b. held the highest lever at 79.48 ± 2.66 %, L.p., L.c., and L.pc. were about the same, while L.a. was the lowest at 50.70 ± 5.93 %. However, the Na^+-K^+-ATPase activity had a different trend with survival rates (Fig. 4b). L.p. and L.a. were at the highest level about 26.48 ± 1.61 and 26.00 ± 0.55 U/mg respectively, while L.b. was at the lowest about 7.26 ± 1.5 U/mg. As for the Ca^{2+}-Mg^{2+}-ATPase activity, it showed the highest in L.a. and the lowest in L.c. at different LAB strains (Fig. 4c). Obviously, adding trehalose to MPN-protected probiotic should be a widely applicable co-protection strategy to LAB starter preparation with great efficiency.

3.5. The storage stability for the probiotic power

The changes of freeze-dried living cells with or without protection during 30-day storage were shown in Fig. 5. We evaluated the impact of different storage temperatures, including −20 °C and 4 °C, on the viability of probiotic powder. After being treated with trehalose and MPN, B.B. maintained the viability of over 10^{10} CFU/mL after 28 days, while the unprotected group only retained 10 % of living cells (Fig. 5a). Probiotic powder activity at 4 °C was lower than at −20 °C. However, regardless of temperature, the survival rate of trehalose and MPN-protected B.B. consistently exceeded 60 % during storage life (Fig. 5b), indicating that the viability far exceeded the industry requirement for 10^7 CFU/mL (L. Liu et al., 2024). Bodzen et al. (2021) designed a new lyoprotectant increasing the survival of freeze-dried *Lactobacillus* strain during long-term storage and the bacterial counts decreased by 0.4 log during storage. Chen et al. (2023) only assessed the freeze-dried powder could be stored stably at −20 °C. H. Yang et al. (2023) showed that heat preadaptation improved the tolerance of *T. halophilus* during freeze-drying, but the survival rate decreased by 76.0 % in the storage time. The result demonstrated that the co-protected method of trehalose and MPN was a good way for B.B. under long-term cryopreservation conditions.

4. Conclusion

In conclusion, our research provides comprehensive information on enhancing viability for probiotics during freeze-drying and addressing critical limitations in traditional preservation methods through the biointerfacial phenolic self-assembly strategy. This study was able to elucidate the effectiveness of enhancing the protection of excipients by MPN in maintaining probiotic vitality after freeze-drying, demonstrating superior post-lyophilization survival rates and outstanding viability in various environmental challenge, such as exposure to antibiotics, extreme acidity and alkalinity, as well as intestinal conditions, and presenting superior shelf life during 30 days of storage. Our results have deepened our understanding of providing mechanistic insights into the role of molecular interactions in probiotic preservation. The protection method, which involves incorporating excipients and using MPN-protected probiotics during freeze-drying, has demonstrated wide

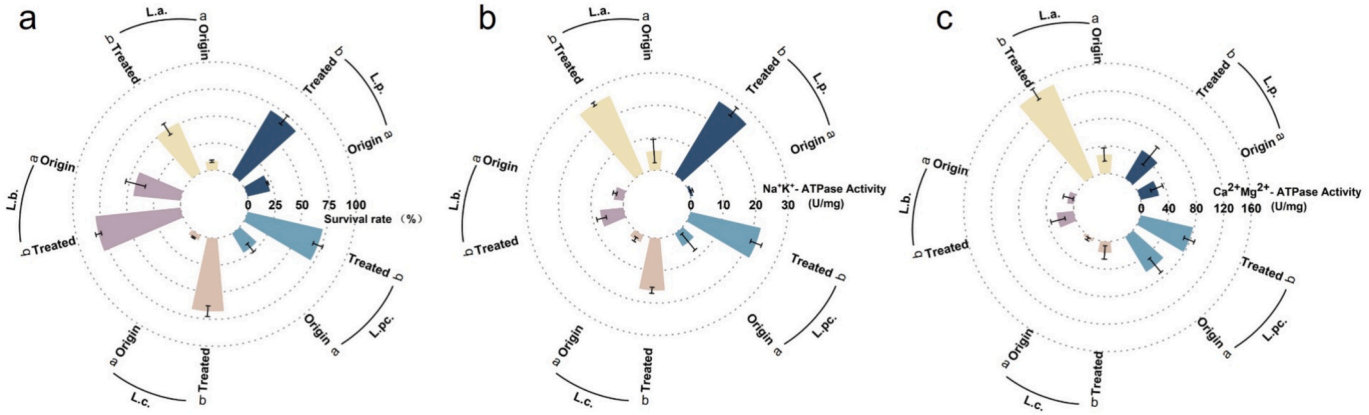

Fig. 4. Cryoprotection of trehalose with MPN for different LAB strains in freeze-drying, (a) indicates survival rate; (b)Na^+-K^+-ATPase activity; and (c) Ca^{2+}-Mg^{2+}-ATPase activity. Significant differences according to Duncan's test ($P < 0.05$) among samples are represented by different lowercase letters.

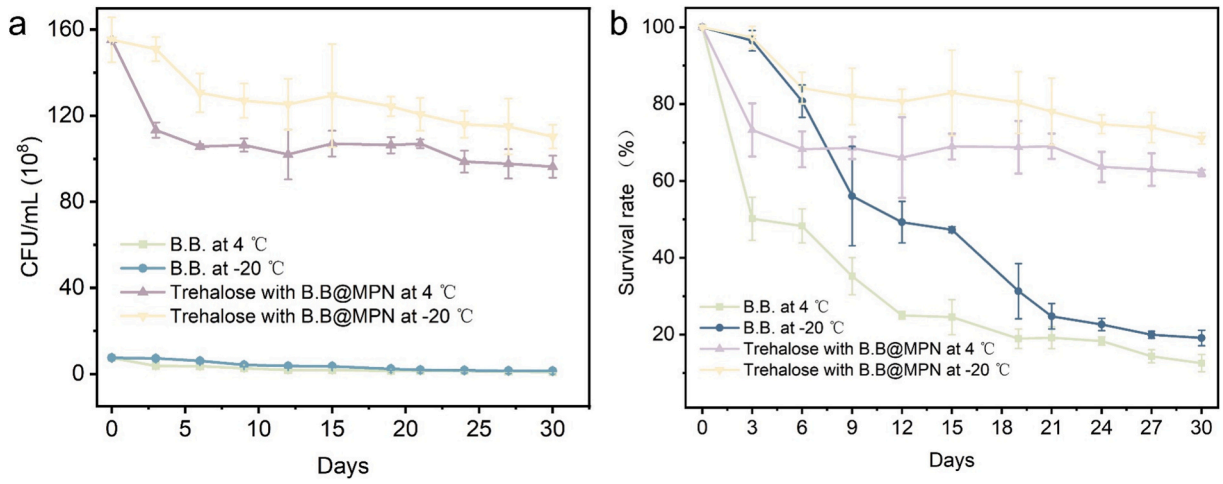

Fig. 5. The storage stability for the probiotic power. The vitality (a) and survival rate (b) of different probiotic powers during 30-day storage.

applicability across diverse probiotic strains. Overall, this strategy is anticipated to tackle the problem of the low survival rate of probiotics following the freeze-drying process and is also a promising way for the long-term preservation of probiotics, fulfilling more potential application requirements for probiotic powder in the future.

CRediT authorship contribution statement

Tong Zhang: Writing – original draft, Software, Methodology, Investigation, Data curation, Conceptualization. **Chen Wang:** Software, Methodology. **Shengpeng Su:** Software, Investigation. **Axiang Sun:** Software. **Ting Du:** Writing – review & editing. **Jianlong Wang:** Supervision. **Julong Liu:** Supervision, Investigation, Conceptualization. **Wentao Zhang:** Writing – review & editing, Funding acquisition.

Declaration of competing interest

The authors declare that they have no known competing financial interests or personal relationships that could have appeared to influence the work reported in this paper.

Acknowledgments

The authors thank the National Key Research and Development Program of China (2023YFE0103300), and Tang Scholar by Cyrus Tang Foundation.

Appendix A. Supplementary data

Supplementary data to this article can be found online at https://doi.org/10.1016/j.foodres.2025.116097.

Data availability

Data will be made available on request.

References

Bodzen, A., Jossier, A., Dupont, S., Mousset, P.-Y., Beney, L., Lafay, S., & Gervais, P. (2021). Design of a new lyoprotectant increasing freeze-dried Lactobacillus strain survival to long-term storage. *BMC Biotechnology, 21*(1), 66.

Chen, B., Wang, X., Li, P., Feng, X., Mao, Z., Wei, J., Lin, X., Li, X., & Wang, L. (2023). Exploring the protective effects of freeze-dried Lactobacillus rhamnosus under optimized cryoprotectants formulation. *LWT, 173*, Article 114295.

Deng, Z., Li, J., Song, R., Zhou, B., Li, B., & Liang, H. (2021). Carboxymethylpachymaran/alginate gel entrapping of natural pollen capsules for the encapsulation, protection and delivery of probiotics with enhanced viability. *Food Hydrocolloids, 120*, Article 106855.

Du, T., Liu, L., Wang, S., Feng, J., Luo, L., Zhang, L., Lan, X., Shen, Y., Shi, S., Wang, J., & Zhang, W. (2024). Molecular-level regulating intersystem crossing of polyphenols: Engineering high-efficiency phytochemical photosensitizer for MRSA elimination. *Nano Today, 58*, Article 102456.

Du, T., Wang, S., Feng, J., Shen, Y., Wang, J., & Zhang, W. (2023). Dual-mechanism tuned engineered polyphenols with Cascade photocatalytic self-Fenton reaction for sustainable biocidal coatings. *Nano Letters, 23*(20), 9563–9570.

Fan, G., Wasuwanich, P., Rodriguez-Otero, M. R., & Furst, A. L. (2022). Protection of Anaerobic Microbes from Processing Stressors Using Metal–Phenolic Networks. *Journal of the American Chemical Society, 144*(6), 2438–2443.

Fenster, K., Freeburg, B., Hollard, C., Wong, C., Rønhave Laursen, R., & Ouwehand, A. C. (2019). The production and delivery of probiotics: A review of a practical approach. *In Microorganisms, 7*.

Ge, S., Han, J., Sun, Q., Zhou, Q., Ye, Z., Li, P., & Gu, Q. (2024). Research progress on improving the freeze-drying resistance of probiotics: A review. *Trends in Food Science & Technology, 147*, Article 104425.

George Kerry, R., Patra, J. K., Gouda, S., Park, Y., Shin, H.-S., & Das, G. (2018). Benefaction of probiotics for human health: A review. *Journal of Food and Drug Analysis, 26*(3), 927–939.

Jia, G., Chen, Y., Sun, A., & Orlien, V. (2022). Control of ice crystal nucleation and growth during the food freezing process. *Comprehensive Reviews in Food Science and Food Safety, 21*(3), 2433–2454.

Kechagia, M. A.-O., Basoulis, D. A.-O. X., Konstantopoulou, S. A.-O., Dimitriadi, D., Gyftopoulou, K., Skarmoutsou, N., & Fakiri, E. A.-O. (2013). Health benefits of probiotics: A review. *ISRN. Nutrition*, 481651 (2314-4068 (Print)).

Kothari, D., Patel, S., & Kim, S.-K. (2019). Probiotic supplements might not be universally-effective and safe: A review. *Biomedicine & Pharmacotherapy, 111*, 537–547.

Li, G., Zhang, Y.-Y., Li, Q., Wang, C., Yu, Y., Zhang, B., … Jiang, L. (2020). Infrared spectroscopic study of hydrogen bonding topologies in the smallest ice cube. *Nature Communications, 11*(1), 5449.

Liu, J., Li, W., Wang, Y., Ding, Y., Lee, A., & Hu, Q. (2021). Biomaterials coating for on-demand bacteria delivery: Selective release, adhesion, and detachment. *Nano Today, 41*, Article 101291.

Liu, L., Xie, S., Zhu, Y., Zhao, H., & Zhang, B. (2024). Sodium carboxymethyl celluloses as a cryoprotectant for survival improvement of lactic acid bacterial strains subjected to freeze-drying. *International Journal of Biological Macromolecules, 260*, Article 129468.

Luo, X., Fan, S., He, Z., Ni, F., Liu, C., Huang, M., Cai, L., Ren, G., Zhu, X., Lei, Q., Fang, W., & Xie, H. (2022). Preparation of alginate-whey protein isolate and alginate-pectin-whey protein isolate composites for protection and delivery of Lactobacillus plantarum. *Food Research International, 161*, Article 111794.

Martins, F. A., Ramalho, T. C., & Freitas, M. P. (2023). Synergistic effect of intra- and intermolecular hydrogen bond in 2-haloethanols probed by infrared. *Spectrochimica Acta Part A: Molecular and Biomolecular Spectroscopy, 288*, Article 122205.

Novak, U., & Grdadolnik, J. (2021). Infrared spectra of hydrogen bond network in lamellar perfluorocarboxylic acid monohydrates. *Spectrochimica Acta Part A: Molecular and Biomolecular Spectroscopy, 253*, Article 119551.

Shi, S., Han, Y., Feng, J., Shi, J., Liu, X., Fu, B., Wang, J., Zhang, W., & Duan, J. (2024). Microenvironment-triggered cascade metal-polyphenolic nanozyme for ROS/NO synergistic hyperglycemic wound healing. *Redox Biology, 73*, Article 103217.

Singh, P., Medronho, B., Alves, L., da Silva, G. J., Miguel, M. G., & Lindman, B. (2017). Development of carboxymethyl cellulose-chitosan hybrid micro- and macroparticles for encapsulation of probiotic bacteria. *Carbohydrate Polymers, 175*, 87–95.

Siri, M., Grasselli, M., & Alonso, S. D. V. (2016). Albumin-based nanoparticle trehalose lyophilisation stress-down to preserve structure/function and enhanced binding. *Journal of Pharmaceutical and Biomedical Analysis, 126*, 66–74.

Tian, Y., He, Z., He, L., Li, C., Qiao, S., Tao, H., Wang, X., Zeng, X., & Tian, Y. (2024). Effect of freeze-dried protectants on the survival rate and fermentation performance of fermented milk's directed vat set starters. *Cryobiology, 114*, Article 104811.

Williams, N. T. (2010). Probiotics. *American Journal of Health-System Pharmacy, 67*(6), 449–458.

Xie, W., Guo, Z., Zhao, L., & Wei, Y. (2021). Metal-phenolic networks: Facile assembled complexes for cancer theranostics. *Theranostics, 11*(6407–6426), 13.

Yang, H., Huang, P., Hao, L., Che, Y., Dong, S., Wang, Z., & Wu, C. (2023). Enhancing viability of dried lactic acid bacteria prepared by freeze drying and spray drying via heat preadaptation. *Food Microbiology, 112*, Article 104239.

Yang, X., Yang, J., Ye, Z., Zhang, G., Nie, W., Cheng, H., … Shi, J. (2022). Physiologically inspired mucin coated Escherichia coli Nissle 1917 enhances biotherapy by regulating the pathological microenvironment to improve intestinal colonization. *ACS Nano, 16*(3), 4041–4058.

Yuan, Y., Yin, M., Chen, L., Liu, F., Chen, M., & Zhong, F. (2022). Effect of calcium ions on the freeze-drying survival of probiotic encapsulated in sodium alginate. *Food Hydrocolloids, 130*, Article 107668.

Zhang, Y., Tang, H., Zheng, Y., Li, J., & Pan, L. (2019). Optimization of ultrasound-assisted extraction of poly-phenols from Ajuga ciliata Bunge and evaluation of antioxidant activities in vitro. *Heliyon, 5*(10), Article e02733.

Zhao, M., Mu, L., Guo, Z., Lv, W., Jiang, H., & Li, B. (2024). Double-layer microcapsules based on shellac for enhancing probiotic survival during freeze drying, storage, and simulated gastrointestinal digestion. *International Journal of Biological Macromolecules, 267*, Article 131483.

International Journal of Biological Macromolecules 308 (2025) 142699

Contents lists available at ScienceDirect

International Journal of Biological Macromolecules

journal homepage: www.elsevier.com/locate/ijbiomac

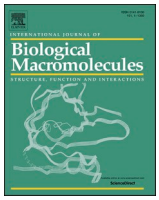

Polydopamine-mediated biointerfacial nanozyme as probiotic protective coating for IBD therapy

Tong Zhang [a,b], Chen Wang [a], Ting Du [a], Haoyu Sun [a], Yaru Han [d], Shuo Shi [c,*], Jianlong Wang [a,*], Wentao Zhang [a,b,**]

[a] College of Food Science and Engineering, Northwest A&F University, Yangling, Shaanxi 712100, China
[b] Northwest A&F University Shenzhen Research Institute, Shenzhen, Guangdong 518000, China
[c] College of Chemistry & Pharmacy, Northwest A&F University, Yangling 712100, Shaanxi, China
[d] Department of Chemical Engineering, Columbia University, New York, NY 10027, USA.

ARTICLE INFO

Keywords:
Probiotics
Nanozyme
Polydopamine

ABSTRACT

Probiotics offer a promising strategy to address the dysfunction of the intestinal mucosal barrier and dysregulation of the gut microbiota in inflammatory bowel disease (IBD). However, the low viability and poor adhesion of probiotics in complex gastrointestinal environments pose significant challenges. To tackle these issues, we designed a specialized protective nano-coating (PDA@CeO_2) using biointerfacial phenolic assembly combined with nanozymes for *Bifidobacterium bifidum* (B.B.). Characteristic peaks of CeO_2 nanoparticles were detected on B.B. via XRD analysis, while SEM and TEM images confirmed the successful attachment of CeO_2 nanoparticles to the probiotic surface. The nano-coating (PDA@CeO_2) simultaneously provides B.B. with high adhesion in the intestine, strong tolerance in complex gastrointestinal environments, and the ability to scavenge excess reactive oxygen species (ROS) due to its excellent mucoadhesive ability and high nanozyme activity. Specifically, the protection provided by nano-coating against simulated gastric fluid (SGF, pH 1.2) resulted in cell survival rates approximately 9.4 times higher than those of unprotected B.B. after 1 h of exposure. In IBD mouse models, the combination of PDA@CeO_2 and B.B. demonstrated excellent therapeutic effects, promoting gut barrier repair. Additionally, an increase in *Muribaculaceae* and *Prevotellaceae_UCG-001* and a decrease in *Desulfovibrionaceae* reshaped the intestinal flora, reducing recurrence. This study highlights the potential of enhancing probiotic functionality through targeted design of protective nano-coatings for IBD therapy.

1. Introduction

Inflammatory bowel disease (IBD) significantly reduces the quality of life of IBD patients and leads to more serious diseases, including colon cancer [1,2]. Current clinical therapies primarily focus on suppressing the intestinal inflammatory burden, however, long-term use of small molecular drugs, antibiotics, and antibodies may lead to numerous adverse reactions. These include antibiotic resistance, immunological responses, and an increased risk of infections and malignant tumors [3–5]. Oral probiotic therapeutics have emerged as strategies for treating IBD due to their superior ability to modulate the balance of the intestinal flora and promote intestinal mucosal repair [6,7]. *Bifidobacterium bifidum* (B.B.) has been shown to relieve IBD in mice potentially by activating the aryl hydrocarbon receptor [8]. However, B. B. is susceptible to reactive oxygen species (ROS) damage in inflammatory bowel diseases (IBDs), lacks adequate adhesion to the intestinal mucosa, and exhibits poor survival in complex gastrointestinal (GI) environments, including strongly acidic gastric fluid, digestive enzymes, and bile salts. Consequently, these factors reduce therapeutic efficacy and prolong the treatment period [9,10]. There is an urgent need for an effective strategy to protect B.B. to treat IBD more effectively and safely.

Currently, methods for protecting probiotics primarily focus on microencapsulation, which involves encapsulating probiotics in hermetically sealed microcapsules. This approach offers significant advantages in improving probiotic viability; however, several challenges remain, including control of particle size, leakage of probiotics, and low in vivo efficiency [11,12]. In contrast to microencapsulation methods, nanoencapsulation of probiotics involves designing protective nano-

* Corresponding authors.
** Correspondence to: W. Zhang, Northwest A&F University Shenzhen Research Institute, Shenzhen, Guangdong 518000, China.
E-mail addresses: shishuo@nwsuaf.edu.cn (S. Shi), wanglong79@nwsuaf.edu.cn (J. Wang), zhangwt@nwsuaf.edu.cn (W. Zhang).

https://doi.org/10.1016/j.ijbiomac.2025.142699
Received 17 October 2024; Received in revised form 26 March 2025; Accepted 29 March 2025
Available online 30 March 2025

coatings around individual probiotic cells to address specific limitations. Consequently, nano-coatings can enhance the ability of probiotics to adhere to and proliferate on intestinal surfaces [12,13]. At present, many researchers have proven the promise of targeted protective nano-coating for probiotics for treating disease, such as a triple immune nanoactivator with polydopamine anchored at the surface of probiotics to inhibit tumors [14], probiotics by camouflaging with cell membrane camouflaged to decrease the inflammatory reaction and side effects [15], and an inorganic nanosheet producing an anti-inflammatory gas shielded probiotics in response to adapt to diverse gastrointestinal microenvironments on-demand, which will hopefully solve the present dilemma for B.B. in IBD therapy [16]. Meanwhile, oral antioxidant nanozymes hold great promise for the treatment of IBD due to their ability to effectively eliminate ROS. However, their practical applications are significantly hindered by the instability of ROS elimination and the potential risk of metal-ion leakage in the digestive tract [17,18].

Here, we designed a nano-coating to help B.B. improve tolerance in GI environments, enhance adhesion in the gut, and treat IBD to reshape the intestinal microenvironment by utilizing phenolic substance self-assembly and electrostatic interactions. The extraordinary adhesive ability of polydopamine (PDA) layers was harnessed through cell-mediated biointerfacial phenolic assembly to coat B.B., thereby improving its adhesion to the intestinal tract and tolerance to harsh GI conditions [19]. Furthermore, CeO_2 nanoparticles (NPs), which function as effective ROS-scavenging enzymes and positively charged materials, were adsorbed onto the PDA layers via electrostatic interactions, endowing probiotics with ROS-scavenging capabilities. Notably, with the protective nano-coating containing PDA and CeO_2 NPs (PDA@-CeO_2), the PDA@CeO_2-coated B.B. (B.B.@PDA@CeO_2) can withstand harsh GI environments. Upon reaching the intestine, B.B.@PDA@CeO_2 efficiently colonizes the colon through the natural adhesion properties of PDA and rapidly enters the logarithmic growth phase. CeO_2 NPs scavenge excess ROS in IBD to inhibit inflammation. Specifically, B.B.@PDA@CeO_2 offers the following advantages: 1) enhanced tolerance to harsh GI environments, 2) improved inherent bioactivity and colonization ability, 3) effective ROS scavenging, and 4) the ability to repair the gut barrier and regulate intestinal flora imbalance. In brief, our findings prove the excellent effects of B.B.@PDA@CeO_2 on IBD therapy. We anticipate that nano-encapsulated bacteria with phenolic substance self-assembly combined with nanozymes could provide a versatile strategy for treating IBDs and protecting any cellular biotherapeutic.

2. Materials and methods

2.1. Materials and chemicals

Bifidobacterium bifidum 6165 was acquired from the Northwest A&F University (Yangling, Shaanxi). The Caco-2 human colon adenocarcinoma cell line was obtained from the Northwest A&F University (Yangling, Shaanxi). Cerium nitrate hexahydrate were purchased from Shanghai Aladdin Biochemical Technology Co., Ltd. (Shanghai, China). Dopamine (DA) was purchased from Shanghai Yuanye Co. Ltd. (Shanghai China).

2.2. Synthesis of polydopamine (PDA) on the surface of probiotics

Different concentrations of dopamine (DA) (0.2, 0.4,0.6, 0.8, and 1 mg/mL) were prepared, added to the bacterial solution, and shaken in a shaker at 37 °C for 1 h [20]. To ensure the optimum concentration of DA, the PDA bacterial solution (B.B.@PDA) was diluted and spread on MRS solid plates. The colonies were counted on plates and compared with the original bacteria (B.B.) that were not coated with PDA. Then, to ensure that the probiotics were encapsulated in the PDA layer, FT-IR spectrometer and Raman spectrum were used to determine the differences between the B.B. and B.B.@PDA surfaces, and scanning electron microscopy (SEM) and transmission electron microscopy (TEM) were used to observe the micromorphology.

2.3. Synthesis of CeO_2 nanoparticles (NPs) on the surface of B.B.@PDA

The synthesis of CeO_2 nanoparticles was based on the method of Zhao, Li, Liu, Li, Cheng, Cheng, Sun, Du, Butch and Wei [17]. 126 mg $Ce(NO_3)_3{\cdot}6H_2O$ crystals were added to 10 mL of polyethylene glycol to form a uniformly dispersed suspension, which was dropped into 10 mL of water and stirred vigorously for 15 min. Then, the above-mixed solution was placed in a water bath at 60 °C and vigorously stirred for 15 min. 28 %–30 % concentrated ammonia solution (3.2 mL) was quickly injected into the mixed solution, and the solution was vigorously stirred for 3 h at 60 °C. Centrifugation and washing with water were repeated until the pH of the supernatant solution became neutral. The synthesized CeO_2 NPs were collected by centrifugation. The final concentration of CeO_2 NPs was 5 mg/mL.

The CeO_2 NPs were linked to the surface of B.B.@PDA by electrostatic interactions. Different ratios of CeO_2 NPs and B.B.@PDA (1:1, 1:2, 1:4, 1:6, and 1:8) were mixed in stasis for 30 min and collected by centrifugation. To determine the optimal mixing ratio, we observed the TEM images. X-ray diffraction (XRD), X-ray photoelectron spectroscopy (XPS), and microbial growth curve were used to ensure CeO_2 NPs linked to the surface of B.B.@PDA.

2.4. The survival rate of B.B.@PDA@CeO_2 in a complex environment

Probiotics with different treatments were dissolved in 30 % ethanol, 50 % ethanol, strong acid (pH = 2), strong base (pH = 11), 30 mM H_2O_2, simulated gastric fluid (SGF pH = 1.2), simulated intestinal fluid (SIF pH = 6.8) and 0.3 mg/mL bile salts at a ratio of 1:1 and then shaken in a shaker at 37 °C and 180 r/min for 1 h. The shaken bacterial solution was centrifuged and resuspended in a sterile 0.9 % NaCl solution. The solution was washed three times. Finally, the colonies were counted on the plates for comparison. We chose trehalose as the cryoprotectant. Probiotics with different treatments were subjected to freeze-drying, and the survival rates were compared with those following the addition of trehalose to ensure a protective effect. The samples were prepared according to Fan, Wasuwanich, Rodriguez-Otero and Furst [21]. And to evaluate the stability of CeO_2 NPs in simulated gastrointestinal environments using the retained activity of SOD-Like and CAT-Like. All treatments exposured to SGF and SIF during 1 h and used SOD-Like and CAT-Like activity detection kit.

2.5. Adhesion assay in Caco-2 cells

The method referred to Centurion and co-workers [20]. For the probiotic inoculation, in all treatments, the concentration of CeO_2 was 0.25 mg/mL, and the concentration of probiotics was 10^8 CFU mL^{-1}. All treatments (100 μL, dispersed in DMEM) were added to 96-well plates containing Caco-2 cells at 37 °C for 2 h, and the cells were detached by trypsinization and mixed to make a homogenous suspension. The cell suspensions were counted using the plate counting method (B_1 CFU mL^{-1}). Probiotic cells initially added to each well of the 96-well plate were also counted (B_0 CFU mL^{-1}). Adhesion rate (%) = $(B_1/B_0) \times 100$.

2.6. DPPH Radical scavenging assay

The DPPH test was based on the method of Blois [22]. Briefly, all samples (1 mL) were added to 0.2 mm DPPH in ethanolic solution (2 mL), stored at 37 °C for 30 min in the dark, and measured at 531 nm. DI water and ethanol (*v*/v 1:2) were used as controls. The antioxidant activity was calculated using the following formula: scavenging effect (%) = (Ac—As)/Ac × 100. Where, As is the absorbance of all treatments and Ac is the absorbance of the control at 531 nm. All these tests were performed in triplicate.

2.7. ROS scavenging ability

First, monolayers of Caco-2 cells were prepared in 24-well plates, and then 10 mM H_2O_2 was used to stimulate the samples for 3 h. After H_2O_2 stimulation, probiotics (dispersed in DMEM) were added to the cells, which were incubated in the dark for 1 h, followed by incubation with 5 μm DCFH-DA in the dark for 10 min. All the cells were subsequently washed with DMEM three times. The culture dishes were transferred to the inverted fluorescent microscope (Leica, Germany), and DCF (2′,7′-dichlorofluorescein) fluorescence was measured with an excitation wavelength of 488 nm and emission at 515–540 nm at the same exposure time [23]. To ensure the fluorescence intensity, cells from monolayers were detached by trypsinization and then measured with the fluorospectro photometer.

To further confirm the in vitro anti-inflammatory effect, murine macrophages (RAW 264.7) were treated with H_2O_2 stimulation. Specifically, all treatments (100 μL, dispersed in DMEM) containing 10 mM H_2O_2 were added to 96-well plates with RAW 264.7 cells and incubated at 37 °C for 2 h. Subsequently, the cells were washed three times with PBS and incubated with 10 μL of MTT solution (1 mg/mL) and 20 μL RPMI medium 1640 for 4 h. Afterward, 100 μL of DMSO was added to each well, followed by a 15-min reaction period. The absorbance at 490 nm was then measured. Cell viability was calculated using the following formula: Cell viability rate (%) = $(A_1/A_0) \times 100$, where A_1 and A_0 represent the absorbance at 490 nm for the sample and control groups, respectively.

2.8. DSS-induced model of IBD

First, the six groups of mice (female, aged 6 to 8 weeks) were given drinking water containing 3 % DSS for 7 days to induce IBD. The body weights of all the mice were recorded daily. Then, one group of mice was given normal drinking water, and the other groups of mice were fed with various treatments including, DSS, B.B., CeO_2 NPs, B.B.@PDA, B.B.@CeO_2, and B.B.@PDA.@CeO_2 (bacteria dose, 1×10^8 CFU; CeO_2 NPs, 2.5 mg/kg) for 6 days. The normal mice (Control) were left untreated throughout the experiment and were given drinking water every day. After that, the mice were euthanized. Colon tissues were harvested and separated into several sections for further analysis, and the colon length was measured. All animal procedures were performed in accordance with the Guidelines for Care and Use of Laboratory Animals of Northwest A&F University and experiments were approved by the Animal Ethics Committee of Northwest A&F University (Approval Number: NWAFAC 1008).

2.9. Histopathology studies

The histopathology analysis for evaluating colon damage was performed according to standard procedures for paraffin embedding and H&E staining. All samples were sent to Servicebio (Wuhan, Hubei).

2.10. MPO assay

The measurement of MPO was based on Liu, Wang, Heelan, Chen, Li and Hu [24]. Briefly, the isolated colon tissues were homogenized in hexadecyltrimethylammonium bromide (0.5 %, $v/w = 5$) in PBS (pH 6.0), freeze-thawed three times (−20 °C ~ 4 °C), sonicated for 10 s, and the supernatant was collected by centrifugation. The supernatant (50 μL) and dianisidine dihydrochloride (200 μL, 1 mg/mL) containing 0.005 % (v/v) H_2O_2 in PBS (pH 6.0) were mixed in a 96-well plate, incubated for 20 min at room temperature, and the OD450 was measured.

2.11. Microbiome analysis

After DSS-induced IBD-bearing mice were subjected to different treatments, the feces were collected on the last day of therapy and prepared for gut microbiome analysis by 16S rRNA sequencing assay. All the samples were sent to the Shenzhen Genomics Institute.

2.12. Statistical analysis

The data were represented as the mean ± standard deviation (SD). The data was analyzed with one-way ANOVA using IBM SPSS 22 statistical software. Duncan's significant difference test evaluated significant differences ($P < 0.05$).

3. Results

3.1. Preparation and characterization of nano-coatings

In our work, we first developed a protective coating on probiotics through biointerfacial phenolic assembly, which triggers the oxidation of dopamine (DA) to polydopamine (PDA). Subsequently, CeO_2 nanoparticles (NPs) were incorporated into the PDA coating via electrostatic interactions, conferring ROS scavenging activity on the probiotics (Fig. 1a). Fig. 1b shows no significant difference in DA concentration between the 0.2–0.4 mg/mL probiotics and the pristine probiotics *(Bifidobacterium bifidum B.B.)*, leading us to select 0.4 mg/mL as the optimal concentration. After determining the DA concentration, we combined PDA with probiotics and analyzed the mixture using FT-IR spectroscopy and Raman spectroscopy. The FT-IR analysis revealed that B.B.@PDA exhibited a characteristic peak at approximately 1630 cm^{-1}, similar to that of individual PDA (Fig. 1c). Meanwhile, the Raman spectrum displayed a dominant band at approximately 1527 cm^{-1}, associated with aromatic functional groups from the PDA layers [20], which was absent in B.B. (Fig. 1d). Scanning electron microscopy (SEM) images revealed that B.B.@PDA had a uniform blocky coating on the surface, while B.B. showed a smooth cell surface (Fig. 1e). Transmission electron microscopy (TEM) images indicated that B.B.@PDA was enveloped in a black film, whereas B.B. lacked this coating. Therefore, we can conclude that the PDA coating had successfully formed on the surface of the probiotics.

Next, we further confirmed the properties of CeO_2 NPs and the relationship between CeO_2 NPs and probiotics. During the growth of probiotics, CeO_2 NPs had a significant negative effect on the probiotics, but the probiotics still maintained a high survival rate (Fig. 1f). The crystalline features of the nanozymes were characterized by using XRD. Our synthesized CeO_2 NPs showed the same characteristic peaks of ceria at $2\theta = 28.5°$, 32.9°, 47.4°, and 56.8° (Figure S1), as shown in Zhao, Li, Liu, Li, Cheng, Cheng, Sun, Du, Butch and Wei [17]. The characteristic peaks of ceria at $2\theta = 28.5°$ and 47.4° were observed for B.B.@CeO_2 and probiotics with PDA coating and CeO_2 NPs (B.B.@PDA@CeO_2), suggesting that CeO_2 NPs were successfully grown on the surface of B.B. (Fig. 2g). The X-ray photoelectron spectroscopy (XPS) results also proved that CeO_2 NPs were present on the surface of B.B.@PDA (Figure S2 and S3). To determine the optimal proportions of B.B. and CeO_2 NPs, we evaluated the TEM results for different mixing ratios of B.B.@CeO_2. We found that probiotics exhibited a uniform surface similar to that of probiotics with CeO_2 NPs (B.B.: CeO_2 NPs 2:1), while B.B.@CeO_2 (1:1) showed that excess CeO_2 NPs and other ratios (4:1, 6:1, and 8:1) all lacked CeO_2 NPs (Figure S4). Of note, B.B.@PDA@CeO_2 shows the delay in exponential growth decreased to 8 h, similar to the study of Fan, Wasuwanich, Rodriguez-Otero and Furst [21]. At last, B.B@PDA@CeO_2 showed that probiotics had been completely encased using CeO_2 NPs (Fig. 1h). The SEM and TEM images of CeO_2 NPs and B.B.@PDA@CeO_2 were shown in Fig. 2i, which confirmed that CeO_2 NPs were successfully linked to the surface of the probiotics. Meanwhile, the results of SEM mapping also illustrated that CeO_2 NPs were present on the surface of B.B.@PDA (Figure S5).

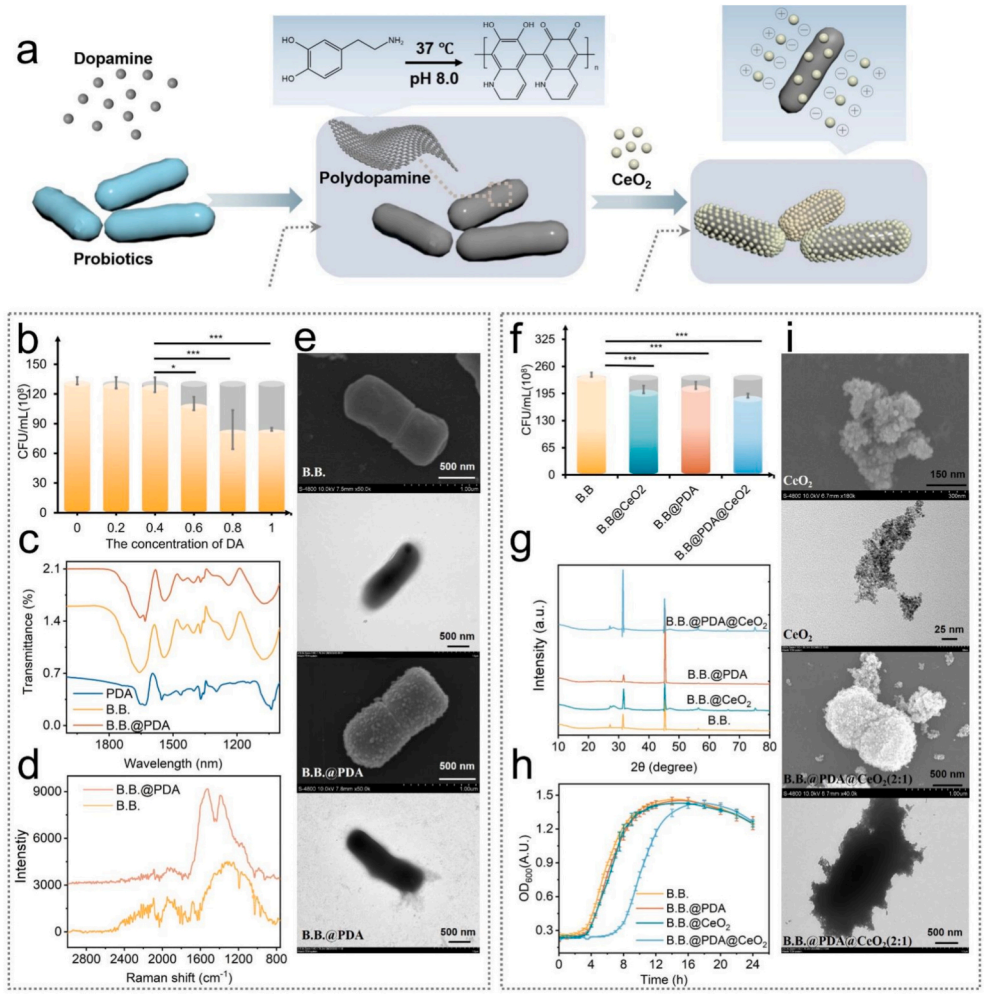

Fig. 1. Preparation and characterization of B.B.@PDA@CeO_2. (a) Schematic illustration of the formation of B.B.@PDA@CeO_2. (b) Effect of the concentration of dopamine (DA) on probiotics. (c) FTIR spectra of PDA, B.B., and B.B.@PDA@CeO_2. (d) Raman spectrum and (e) SEM and TEM images of B.B. and B.B.@PDA. (f) Effect of the addition of CeO_2 to probiotics. (g) XRD and (h) growth curves of B.B., B.B.@CeO_2, B.B.@PDA, and B.B.@PDA@CeO_2. (i) SEM and TEM images of CeO_2 and B.B.@PDA@CeO_2. Error bars represent the standard deviation ($n = 3$). Significant differences according to Duncan's test. $^*P < 0.05$, $^{**}P < 0.01$, $^{***}P < 0.001$. n. s., not significant.

3.2. Tolerance to complex environments

Probiotics offer numerous benefits but are highly susceptible to inactivation by various antibacterial chemicals, including strong acids, bases, and ethanol. We investigated the effect of nano-coating on the survival of probiotics in the presence of these antibacterial agents. In strongly acidic and alkaline environments, B.B.@PDA@CeO_2 exhibited growth trends similar to those observed under ethanol exposure (Fig. 2a and b). Moreover, the survival rate of PDA-coated B.B. was significantly higher than that of uncoated B.B., which can be attributed to the in-situ synthesis of a nano-film on the probiotic surface using interfacial manganese as a catalyst. However, electrostatic deposition of CeO_2 on the probiotic surface may result in an uneven distribution of the coating. Dry storage is often necessary for the administration of microbes, and lyophilization is commonly used for this purpose [25]. Therefore, bacterial counts were monitored before and after lyophilization in liquid medium. Impressively, B.B.@PDA@CeO_2 demonstrated significantly higher bacterial counts compared to B.B. in phosphate citrate (PC) buffer. To further evaluate the protective effect of B.B.@PDA@CeO_2 during lyophilization, we compared it with common cryoprotectants such as trehalose. Fig. 2c shows that the bacterial counts of B.B@PDA@CeO_2 had no significant difference compared with probiotics supplemented with trehalose. As shown in Fig. 2d and e, more coated probiotics survived after 1 h of exposure to 30 % and 50 % ethanol compared with uncoated probiotics, with B.B.@PDA@CeO_2 having the highest survival rate, which was nearly 10 times higher than that of uncoated probiotics. Meanwhile, we evaluated the tolerance probiotics to H_2O_2, as shown in Fig. 2f, which also exhibited that B.B.@PDA@CeO_2 had the highest survival rate.

We considered that the survival of probiotics in low gastric pH environments is a functional requirement for their gastrointestinal transit processes [26]. We subsequently investigated the effect of the nano-coating on the survival and growth of B.B. in simulated gastrointestinal (GI) environments, including simulated gastric fluid (SGF), simulated intestinal fluid (SIF), and 0.3 mg/mL bile salts. The protection conferred by B.B.@PDA@CeO_2 against SGF (pH 1.2) resulted in cell survival approximately 9.4 times higher than that of B.B. after 1 h of exposure. The survival of B.B. with nano-coating increased as the coating content increased (Fig. 2g). A similar trend was observed for SIF and bile salts. As shown in Fig. 2h and i, B.B.@PDA@CeO_2 exhibited the highest bacterial count compared to other treatments, particularly under bile salt conditions. Compared to B.B., B.B.@PDA@CeO_2 demonstrated significantly greater tolerance to these simulated GI environments. To evaluate the stability of CeO_2 nanoparticles (NPs) in simulated GI environments, we assessed the retained activity of SOD-like and CAT-like enzymes after 1 h of exposure to SGF and SIF (**Figs. S6 and S7**). The

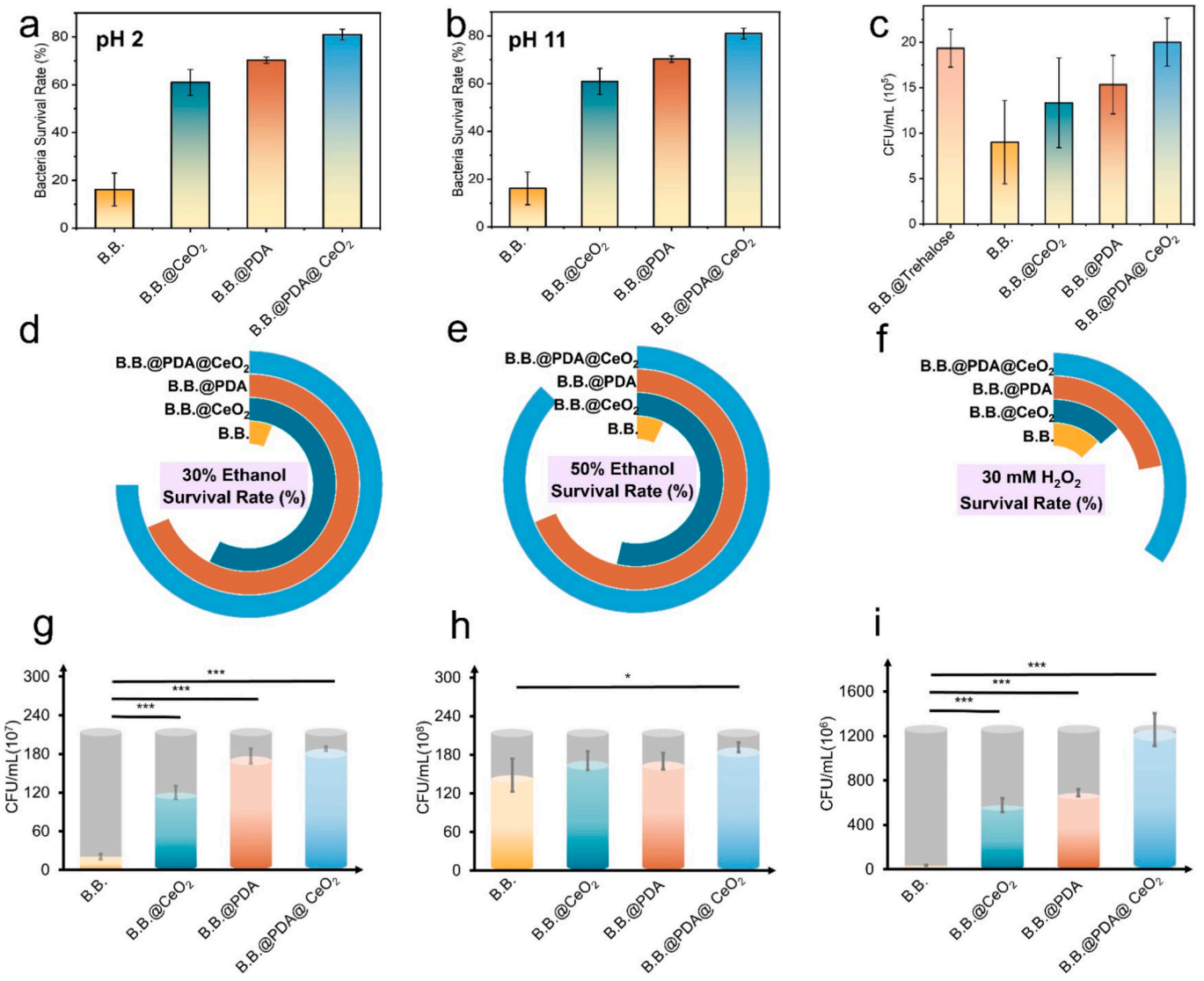

Fig. 2. The survival rate of different treatments at (a) pH = 2, (b) pH = 11, (c) lyophilization, (d) 30 % ethanol, (e) 50 % ethanol, and (f) 30 mM H_2O_2. The bacterial counts of different treatments in (g) SGF (pH 1.2), (h) SIF (pH 6.8) at 37 °C, and (i) 0.3 mg/mL bile salts. Error bars represent the standard deviation (n = 3). Significant differences according to Duncan's test. *P < 0.05, **P < 0.01, ***P < 0.001. n.s., not significant.

results indicated that the retained activity remained almost unchanged in both SGF and SIF. These findings demonstrated that the combination of the PDA layer with CeO_2 NPs significantly enhances the tolerance of probiotics to complex environments.

3.3. Cell adhesion and ROS scavenging abilities of B.B.@PDA@CeO_{2a}

The adherence of probiotics to the host intestine has been shown to increase their transit time in the gut, thus enhancing their beneficial properties [27]. The overproduction of reactive oxygen species (ROS) is the major cause of intestinal inflammation [7]. However, survival in the presence of ROS and mucoadhesion and colonization by probiotics are still difficult, so we further evaluated the cell adhesion and ROS scavenging abilities of B.B.@PDA@CeO_2 in Caco-2 cells (Fig. 3a). As shown in Fig. 3b, the adhesion rate of B.B.@PDA@CeO_2 was 93.36 %, while that of B.B. was only 20.46 %. The adhesion rate of the cells coated with CeO_2 NPs was greater than that of the cells coated with uncoated CeO_2 NPs because the CeO_2 NPs targeted the cells via electrostatic interactions. Therefore, B.B.@PDA@CeO_2 had superior adhesion to Caco-2 cells. Antioxidants play a critical role in lowering the risk of disease by reducing oxidative stress [28]. Thus, inspired by the natural antioxidant activity of phenolic compounds, CeO_2 NPs have excellent anti-ROS effects [17,29], so we evaluated their ability to scavenge DPPH radicals in vitro (Fig. 3c). Compared with B.B., B.B. with a nano-coating exhibited greater scavenging activity, of which B.B.@PDA@CeO_2 had the highest activity. Most bowel diseases, such as IBD, can produce excessive reactive oxygen species (ROS) [18]. Various nanozymes have been developed for the treatment of IBD, and CeO_2 NPs have been shown to have excellent ROS scavenging ability [17]. Then, we evaluated the ROS-scavenging ability of B.B.@PDA@CeO_2. As shown in Fig. 3d and e, after treatment with 10 mM H_2O_2, the H_2O_2 group exhibited high fluorescence intensity, indicating oxidative stress, and the cellular state deteriorated accordingly. In contrast, the fluorescence intensity of B.B.@PDA@CeO_2 was markedly lower than that of other probiotic treatments (Fig. 3d), a result further corroborated by Fig. 3e. Notably, fluorescence imaging revealed no significant difference between the Control group and the B.B.@PDA@CeO_2 group. Subsequently, we assessed the effects of different H_2O_2 stimulation treatments on cell viability in murine macrophages (RAW 264.7). As depicted in **Figure S8**, B.B.@PDA@CeO_2 demonstrated the highest cell viability among all treatments. Therefore, the combination of the PDA layer with CeO_2 nanoparticles (NPs) substantially enhanced the ROS-scavenging capacity of

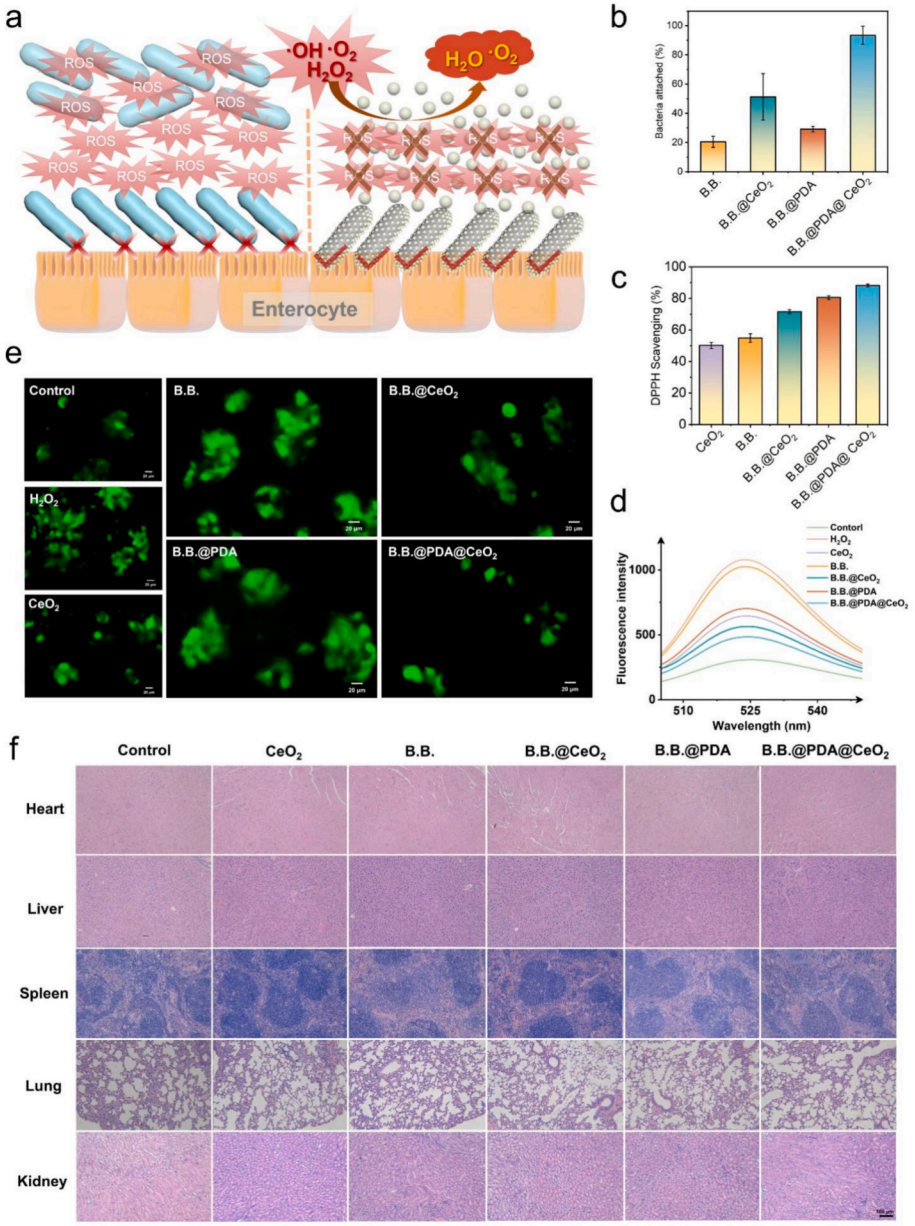

Fig. 3. (a) Schematic illustration of the advantages of B.B.@PDA@CeO_2 in cell assays. (b) The adhesion rate in Caco-2 cells and (c) the DPPH scavenging rate of different treatments. (d) Fluorescence spectra and (e) changes in fluorescence microscopes (Scale bar, 20 μm) of different treatments in ROS scavenging tests. (f) Organ slices after different treatments (Scale bar, 100 μm). Error bars represent the standard deviation (n = 3).

probiotics. To evaluate material safety, histological analysis of major organs from treated mice showed no morphological changes compared to untreated mice (Fig. 3f), suggesting the biocompatibility and safety of CeO_2 NPs, probiotics, and the PDA layer.

3.4. *Therapeutic efficacy of B.B.@PDA@CeO_2 against IBD*

To determine the therapeutic efficacy of B.B.@PDA@CeO_2 against IBD, we developed the mouse IBD model by feeding 3 % DSS to mice for 6 days without treatment (Fig. 4a**)**. Afterward, the DSS treatment was discontinued, and different treatments (bacteria dose, 1×10^8 CFU mL^{-1}; CeO_2 NPs, 2.5 mg/mL), including B.B., CeO_2 NPs, B.B. combined with PDA (B.B.@PDA), B.B. combined with CeO_2 NPs (B.B. @CeO_2), and B.B. combined with PDA and CeO_2 NPs (B.B.@PDA@CeO_2), were fed for six consecutive days. The positive control mice (DSS) were treated with PBS, and the negative control mice (Control) were not treated with DSS. The mice colons were isolated and imaged, as a reduction in colon length is typical of the deleterious inflammatory response induced by IBD. As shown in Fig. 4b and d, the colons were all longer in all treatment groups than the DSS treatment, and the colon length of the B.B.@PDA@CeO_2 showed no significant differences compared with the Control treatment. The changes in body weight reflected the severity of IBD. All treatment groups displayed increased body weight after 6 days (**Figure S9**). The body weights of all the groups containing PDA and CeO_2 NPs displayed similar trends on day 5. Notably, B.B.@PDA@CeO_2 had the highest weight in comparison with the other treatments, and the initial body weight of mice treated with B.B.@PDA@CeO_2 almost fully recovered after 5 days, demonstrating the potent therapeutic efficacy of B.B. combined with nano-coating against IBD. The disease activity index (DAI) scores exhibited the same results (**Figure S10**). The assessment of DAI is shown in **Table S1**.

Representative images and histological scores are shown in Fig. 4c and e. Severe damage to the colon, such as a complete loss of crypts, goblet cell depletion, and immune cell infiltration, was observed in the

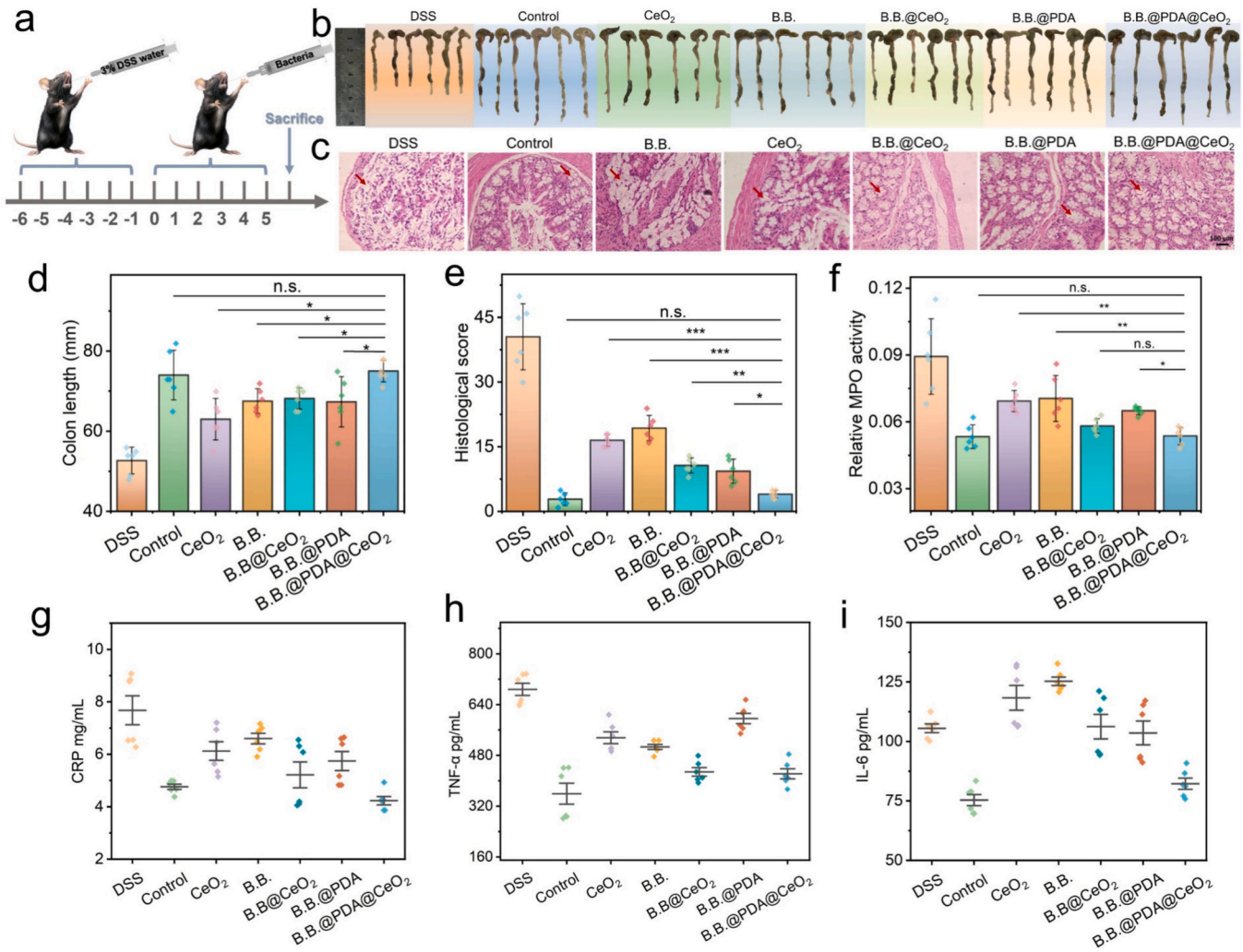

Fig. 4. (a)Schematic of the treatment plan. The mice were induced with the IBD with 3 % DSS from days 0 to 7. Afterward, different formulations were given to the mice for 5 days. (b) Colon images in different groups (The red arrow represents the changes of goblet cells). (c) Images of H&*E*-stained colon tissue (Scale bar, 100 μm). (d) The comparison of colon length in different treatments. (e) Histopathology scores of different treatments. (f) Relative MPO activity in colon tissues of different treatments to measure the inflammation in the colon. Inflammatory factors include (g) CRP, (h) TNF-α, and (i) IL-6 in colon tissues measured by commercially available ELISA kits. Error bars represent the standard deviation ($n = 6$). Significant differences according to Duncan's test. *P < 0.05, **P < 0.01, ***P < 0.001. n.s., not significant.

DSS group (Fig. 4c), whereas substantial improvements were found in the treatment groups. This improvement in the B.B.@PDA@CeO_2 group was especially substantial, as the B.B.@PDA@CeO_2 group exhibited an almost intact epithelial layer and negligible inflammatory cell infiltration. Moreover, the histological scoring guidelines for DSS-induced IBD are shown in Table S2 [30]. The histological score for B.B.@PDA@CeO_2 was significantly lower than that for the other treatments (Fig. 4e).

Next, colonic myeloperoxidase (MPO) activity was evaluated for the level of inflammation in the colon tissues because MPO is a marker of neutrophil activity. As shown in Fig. 4f, the MPO activity of the B.B.@PDA@CeO_2 group showed no significant difference compared to the Control and B.B.@CeO_2 groups, and significantly lower than the CeO_2 group, indicating that the combination of CeO_2 NPs with B.B. was beneficial for the ability of CeO_2 NPs to scavenge ROS in IBD therapy. The MPO activity in the other treatment groups was significantly higher than that in the B.B.@PDA@CeO_2 group. The levels of inflammatory factors, including interleukin-6 (IL-6), C-reactive protein (CRP), and tumor necrosis factor–α (TNF-α), in serum collected from mice were evaluated using commercially available enzyme-linked immunosorbent assay (ELISA) kits. Compared with those in the control group, the inflammatory responses of the B.B., B.B.@ CeO_2, B.B.@PDA, and B.B.@PDA@CeO_2 groups were alleviated, and the inflammatory response of the B.B.@PDA@CeO_2 group returned to normal levels (Fig. 4**, g to i**). As a result, the B.B.@PDA@CeO_2 group demonstrated the excellent therapeutic effect in treating IBD.

3.5. *Modulatory effect of B.B.@PDA@CeO_2 on the gut microbiome*

Due to the ability of probiotics to modulate the gut microbiota and have a beneficial effect on the body, the composition of the gut microbiota is altered by various treatments [31,32]. The feces were collected after treatment treatments with various formulations for 4 days and analyzed via a 16S ribosomal RNA (rRNA) gene sequencing assay. The bacterial richness, presented as observed operational taxonomic units (OTUs), is shown in Fig. 5a. OTUs of all containing B.B. treatments were significantly higher than that in the DSS group, indicating the beneficial effects on gut microbiota modulation for B.B., and OTUs of the B.B.@PDA@CeO_2 group were remarkably highest than that of others containing B.B. groups and Control group, which further illustrated that the nano-coating helped the B.B. have a better effect on modulating bacterial richness. In addition, the Shannon (Fig. 5b) and inverse-Simpson indices (Fig. 5c) were used to determine the α-diversity of the gut

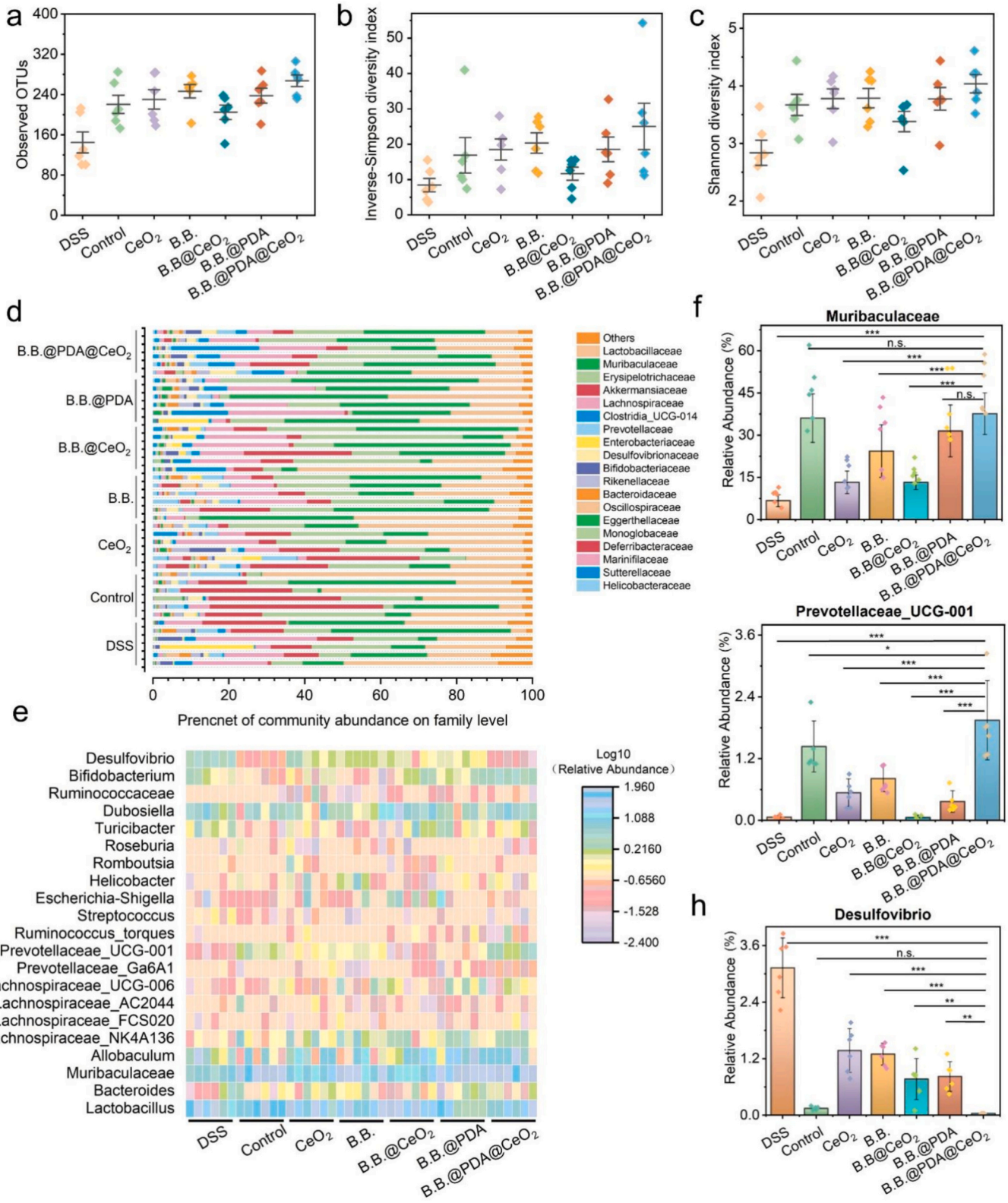

Fig. 5. In the analysis of the gut microbiota, (a) operational taxonomic unit (OTU) richness, (b) inverse-Shannon diversity index, and (c) Shannon index under different treatments. (d) Relative abundance of the gut microbiome at the family level in the different groups. (e) Heatmap illustration of the relative abundance of gut microbes at the genus level in different groups. Relative abundances of (f)*Muribaculaceae*, (g) *Prevotellaceae_UCG-001*, and (h) *Desulfovibrionaceae* in the different groups. Error bars represent the standard deviation (n = 6). Significant differences according to Duncan's test. *P < 0.05, **P < 0.01, ***P < 0.001. n.s., not significant.

microbiome. The abundances of B.B.@PDA@CeO_2 and B.B.@PDA were remarkably higher than those in the B.B. group because the protective and adhesive capacity of the PDA layer increased the abundance of B.B. in the gut. In addition, β-diversity analysis of the gut microbiome using principal coordinate analysis plots revealed that the gut microbiota profiles of the mice in the B.B.@PDA@CeO_2 group differed from those in the other groups. (**Figure S11**). Next, we further investigated the family (Fig. 5d) and genus (Fig. 5e) levels to specifically reveal the content of the gut microbiota in all the groups. *Muribaculaceae* is known to regulate inflammatory responses [33] and *Prevotellaceae_UCG-001* is known to produce short-chain fatty acids [34], which are important and beneficial components of the intestinal flora. As shown in **Fig. 5f and g,** B.B. @PDA@CeO_2 significantly increased the relative abundance of beneficial bacteria compared to that in the other treatment groups and the *Muribaculaceae* of B.B.@PDA@CeO_2 had no significant difference in comparison with the Control group, while the beneficial bacteria prominently decreased in the DSS group. Moreover, *Desulfovibrionaceae*, a virulent pathogen that would worsen IBD, had been known to produce lipopolysaccharides to damage the gut barrier [35]. Fig. 5h shows that the relative abundance of *Desulfovibrionaceae* in all groups containing B. B., PDA, and CeO_2 was markedly reduced, therefore, the relative abundance of Desulfovibrionaceae in the B.B.@PDA@CeO_2 was minimal compared to that in other groups. These results proved that B.B. @PDA@CeO_2 had an up-regulative effect on the intestinal gut microbiota. Compared with those of the other treatments, B.B.@PDA@CeO_2 of the relative abundance of *Bifidobacterium* was highest (**Figure S12**), further showing the protective and colonized effect of our nano-coating on probiotics.

4. Discussion and conclusion

We developed a strategy to protect B.B. and enhance its functions to adapt to the intestinal microenvironment of IBD. A safe and protective nano-coating (PDA@CeO_2) for B.B. was prepared and characterized. All results confirmed that the nano-coating had successfully formed on the surface of B.B. Compared with other groups, the B.B.@PDA@CeO_2 group exhibited superior tolerance to various complex environments. This enhanced resilience is likely attributed to the uniform nano-coating on individual cells, which protects B.B. from environmental assaults. The efficient antioxidant properties of B.B.@PDA@CeO_2 can be explained by the synergistic effects of PDA and CeO_2 nanoparticles in scavenging free radicals. Additionally, the excellent adhesion properties of PDA contribute to the overall stability and effectiveness of the coating [20]. Moreover, B.B.@PDA@CeO_2 better ROS scavenging ability in the microenvironment during IBD therapy due to the presence of the multi-enzymatic nanozyme including SOD- and CAT-like activities [36].

In the mouse colitis model, the extent of colon damage serves as a critical indicator for evaluating IBD therapy. Representative images and histological scores revealed that the colon damage in the B.B.@PDA@-CeO_2 group was minimal and not significantly different from that of the control group, demonstrating the superior therapeutic effect of combining B.B. with the nano-coating. Additionally, the levels of inflammatory factors and MPO activity further confirmed the anti-inflammatory efficacy of B.B.@PDA@CeO_2 [24]. According to the analysis of the gut microbiota, B.B.@PDA@CeO2 was capable of positively modulating the abundance of beneficial bacteria, significantly reducing the abundance of pathogens, and enhancing both the abundance and diversity of the gut microbiome. This contributed to the regulation of gut microbiota dysbiosis, thereby achieving excellent therapeutic efficacy for IBD treatment [35,37].

In summary, given the complex living environment in the delivery system and the harsh intestinal disease environment for probiotics, we designed a platform that enhances the excellent tolerance of B.B. in harsh gastrointestinal (GI) environments, its extraordinary adhesion in the intestine, and its capacity to scavenge reactive oxygen species (ROS). This was achieved by leveraging the self-assembly of phenolics on the surface of B.B. and electrostatically combining CeO_2 nanoparticles (NPs). Compared with the original probiotics, B.B.@PDA@CeO_2 exhibited superior tolerance in complex environments and enhanced adhesion. Moreover, the synergistic effect of B.B.@PDA@CeO_2 in simultaneously scavenging ROS and modulating microbiota homeostasis in the colonic microenvironment significantly improved therapeutic efficacy against DSS-induced IBD. In this study, B.B.@PDA@CeO_2 demonstrated excellent safety in mouse models; however, further evaluation is necessary before clinical application. Overall, the designed nano-coating protected the probiotics and enhanced their functionality. The use of a nanozyme-coated probiotic increased activity compared to using a single nanozyme alone. This strategy holds promise for addressing existing limitations in oral probiotic therapeutics for IBD.

CRediT authorship contribution statement

Tong Zhang: Writing – original draft, Software, Methodology, Investigation, Conceptualization. **Chen Wang:** Software, Methodology, Investigation. **Ting Du:** Writing – review & editing, Software. **Haoyu Sun:** Software, Methodology. **Yaru Han:** Supervision. **Shuo Shi:** Investigation, Funding acquisition. **Jianlong Wang:** Writing – review & editing, Investigation, Conceptualization. **Wentao Zhang:** Writing – review & editing, Supervision, Funding acquisition, Conceptualization.

Declaration of competing interest

The authors declare that they have no known competing financial interests or personal relationships that could have appeared to influence the work reported in this paper.

Acknowledgments

The authors thank National Science Foundation of China (31901794), the Macau Young Scholars Program (AM2022021), the National Postdoctoral Program for Innovative Talents (BX20180263), National Key Research and Development Program of China (2023YFE0103300), GuangDong Basic and Applied Basic Research Foundation (2024A1515030053), China Postdoctoral Science Foundation (2023 M732884), Shaanxi Postdoctoral Science Foundation (2023BSHYDZZ68, 2023BSHYDZZ67), and Tang Scholar by Cyrus Tang Foundation.

Appendix A. Supplementary data

Supplementary data to this article can be found online at https://doi.org/10.1016/j.ijbiomac.2025.142699.

Data availability

Data will be made available on request.

References

[1] S. Alatab, S.G. Sepanlou, K. Ikuta, H. Vahedi, C. Bisignano, S. Safiri, A. Sadeghi, M. R. Nixon, A. Abdoli, H. Abolhassani, V. Alipour, M.A.H. Almadi, A. Almasi-Hashiani, A. Anushiravani, J. Arabloo, S. Atique, A. Awasthi, A. Badawi, A.A. A. Baig, N. Bhala, A. Bijani, A. Biondi, A.M. Borzì, K.E. Burke, F. Carvalho, A. Daryani, M. Dubey, A. Eftekhari, E. Fernandes, J.C. Fernandes, F. Fischer, A. Haj-Mirzaian, A. Haj-Mirzaian, A. Hasanzadeh, M. Hashemian, S.I. Hay, C. L. Hoang, M. Househ, O.S. Ilesanmi, N. Jafari Balalami, S.L. James, A.P. Kengne, M. M. Malekzadeh, S. Merat, T.J. Meretoja, T. Mestrovic, E.M. Mirrakhimov, H. Mirzaei, K.A. Mohammad, A.H. Mokdad, L. Monasta, I. Negoi, T.H. Nguyen, C. T. Nguyen, A. Pourshams, H. Poustchi, M. Rabiee, N. Rabiee, K. Ramezanzadeh, D. L. Rawaf, S. Rawaf, N. Rezaei, S.R. Robinson, L. Ronfani, S. Saxena, M. Sepehrimanesh, M.A. Shaikh, Z. Sharafi, M. Sharif, S. Siabani, A.R. Sima, J. A. Singh, A. Soheili, R. Sotoudehmanesh, H.A.R. Suleria, B.E. Tesfay, B. Tran, D. Tsoi, M. Vacante, A.B. Wondmieneh, A. Zarghi, Z.-J. Zhang, M. Dirac, R. Malekzadeh, M. Naghavi, The global, regional, and national burden of inflammatory bowel disease in 195 countries and territories, 1990–2017: a

systematic analysis for the global burden of disease study 2017, the lancet, Gastroenterol. Hepatol. 5 (1) (2020) 17–30.
[2] M.L. Hoivik, B. Moum, I.C. Solberg, M. Cvancarova, O. Hoie, M.H. Vatn, T. Bernklev, f.t.I.S. Group, Health-related quality of life in patients with ulcerative colitis after a 10-year disease course: results from the IBSEN study, Inflamm. Bowel Dis. 18 (8) (2012) 1540–1549.
[3] C.N. Bernstein, M. Fried, J.H. Krabshuis, H. Cohen, R. Eliakim, S. Fedail, R. Gearry, K.L. Goh, S. Hamid, A.G. Khan, A.W. LeMair, Q. Malfertheiner, J.F. Ouyang, A. Rey, F. Sood, O.O. Steinwurz, A. Thomsen, G. Watermeyer Thomson, World gastroenterology organization practice guidelines for the diagnosis and management of IBD in 2010, Inflamm. Bowel Dis. 16 (1) (2010) 112–124.
[4] C. Lautenschläger, C. Schmidt, D. Fischer, A. Stallmach, Drug delivery strategies in the therapy of inflammatory bowel disease, Adv. Drug Deliv. Rev. 71 (2014) 58–76.
[5] A. Stallmach, S. Hagel, T. Bruns, Adverse effects of biologics used for treating IBD, best Practice & Research Clinical, Gastroenterology 24 (2) (2010) 167–182.
[6] X. Wang, Z. Cao, M. Zhang, L. Meng, Z. Ming, J. Liu, Bioinspired oral delivery of gut microbiota by self-coating with biofilms, Sci. Adv. 6 (26) (2020) eabb1952.
[7] J. Zhou, M. Li, Q. Chen, X. Li, L. Chen, Z. Dong, W. Zhu, Y. Yang, Z. Liu, Q. Chen, Programmable probiotics modulate inflammation and gut microbiota for inflammatory bowel disease treatment after effective oral delivery, Nat. Commun. 13 (1) (2022) 3432.
[8] Q.-y. Cui, X.-y. Tian, X. Liang, Z. Zhang, R. Wang, Y. Zhou, H.-x. Yi, P.-m. Gong, K. Lin, T.-j. Liu, L.-w. Zhang, Bifidobacterium bifidum relieved DSS-induced colitis in mice potentially by activating the aryl hydrocarbon receptor, Food Funct. 13 (9) (2022) 5115–5123.
[9] B.P. Abraham, E.M.M. Quigley, Probiotics in inflammatory bowel disease, Gastroenterol. Clin. N. Am. 46 (4) (2017) 769–782.
[10] Z. Cao, X. Wang, Y. Pang, S. Cheng, J. Liu, Biointerfacial self-assembly generates lipid membrane coated bacteria for enhanced oral delivery and treatment, Nat. Commun. 10 (1) (2019) 5783.
[11] T.W. Yeung, I.J. Arroyo-Maya, D.J. McClements, D.A. Sela, Microencapsulation of probiotics in hydrogel particles: enhancing Lactococcus lactis subsp cremoris LM0230 viability using calcium alginate beads, Food Funct. 7 (4) (2016) 1797–1804.
[12] F. Centurion, A.W. Basit, J. Liu, S. Gaisford, M.A. Rahim, K. Kalantar-Zadeh, Nanoencapsulation for probiotic delivery, ACS Nano 15 (12) (2021) 18653–18660.
[13] A.C. Anselmo, K.J. McHugh, J. Webster, R. Langer, A. Jaklenec, Layer-by-layer encapsulation of probiotics for delivery to the microbiome, Adv. Mater. 28 (43) (2016) 9486–9490.
[14] J. Li, Q. Xia, H. Guo, Z. Fu, Y. Liu, S. Lin, J. Liu, Decorating Bacteria with triple immune Nanoactivators generates tumor-resident living Immunotherapeutics, Angew. Chem. 134 (27) (2022) e202202409.
[15] Z. Cao, S. Cheng, X. Wang, Y. Pang, J. Liu, Camouflaging bacteria by wrapping with cell membranes, Nat. Commun. 10 (1) (2019) 3452.
[16] Y.-X. Zhu, Y. You, Z. Chen, D. Xu, W. Yue, X. Ma, J. Jiang, W. Wu, H. Lin, J. Shi, Inorganic Nanosheet-shielded probiotics: a self-adaptable Oral delivery system for intestinal disease treatment, Nano Lett. 23 (10) (2023) 4683–4692.
[17] S. Zhao, Y. Li, Q. Liu, S. Li, Y. Cheng, C. Cheng, Z. Sun, Y. Du, C.J. Butch, H. Wei, An orally administered CeO2@montmorillonite Nanozyme targets inflammation for inflammatory bowel disease, Therapy 30 (45) (2020) 2004692.
[18] Q. Huang, Y. Yang, Y. Zhu, Q. Chen, T. Zhao, Z. Xiao, M. Wang, X. Song, Y. Jiang, Y. Yang, J. Zhang, Y. Xiao, Y. Nan, W. Wu, K. Ai, Oral metal-free melanin Nanozymes for natural and durable targeted treatment of inflammatory bowel disease (IBD), Small 19 (19) (2023) 2207350.
[19] W. Cheng, X. Zeng, H. Chen, Z. Li, W. Zeng, L. Mei, Y. Zhao, Versatile Polydopamine platforms: synthesis and promising applications for surface modification and advanced nanomedicine, ACS Nano 13 (8) (2019) 8537–8565.
[20] F. Centurion, S. Merhebi, M. Baharfar, R. Abbasi, C. Zhang, M. Mousavi, W. Xie, J. Yang, Z. Cao, F.-M. Allioux, G.F.S. Harm, J. Biazik, K. Kalantar-Zadeh, M. A. Rahim, Cell-mediated biointerfacial phenolic assembly for probiotic Nano encapsulation, Adv. Funct. Mater. 32 (26) (2022) 2200775.
[21] G. Fan, P. Wasuwanich, M.R. Rodriguez-Otero, A.L. Furst, Protection of Anaerobic Microbes from Processing Stressors Using Metal–Phenolic Networks, J. Am. Chem. Soc. 144 (6) (2022) 2438–2443.
[22] M.S. Blois, Antioxidant determinations by the use of a stable free radical, Nature 181 (4617) (1958) 1199–1200.
[23] N.K. Lee, Y.G. Choi, J.Y. Baik, S.Y. Han, D.-w. Jeong, Y.S. Bae, N. Kim, S.Y. Lee, A crucial role for reactive oxygen species in RANKL-induced osteoclast differentiation, Blood 106 (3) (2005) 852–859.
[24] J. Liu, Y. Wang, W.J. Heelan, Y. Chen, Z. Li, Q. Hu, Mucoadhesive probiotic backpacks with ROS nanoscavengers enhance the bacteriotherapy for inflammatory bowel diseases, science, Advances 8 (45) (2022) eabp8798.
[25] Y. Miyamoto-Shinohara, T. Imaizumi, J. Sukenobe, Y. Murakami, S. Kawamura, Y. Komatsu, Survival rate of microbes after freeze-drying and long-term storage, Cryobiology 41 (3) (2000) 251–255.
[26] N. Rokana, B.P. Singh, N. Thakur, C. Sharma, R.D. Gulhane, H. Panwar, Screening of cell surface properties of potential probiotic lactobacilli isolated from human milk, J. Dairy Res. 85 (3) (2018) 347–354.
[27] K. Wang, Q. Chen, L. Ding, Y. Zhu, X. Wang, M. Zhou, M. Chang, M. Pei, Y. Zhang, Y. Zhang, Y. Chen, H. Qin, Mucoadhesive probiotic-based oral microcarriers with prolonged intestinal retention for inflammatory bowel disease therapy, Nano Today 50 (2023) 101876.
[28] T. Feng, J. Wang, Oxidative stress tolerance and antioxidant capacity of lactic acid bacteria as probiotic: a systematic review, Gut Microbes 12 (1) (2020) 1801944.
[29] P.B. Singh, A. Young, A. Homayouni, L.H. Hove, B.É. Petrovski, B.B. Herlofson, Ø. Palm, M. Rykke, J.L. Jensen, Distorted taste and impaired Oral health in patients with sicca complaints, Nutrients 11 (2) (2019) 264.
[30] P. Praveschotinunt, A.M. Duraj-Thatte, I. Gelfat, F. Bahl, D.B. Chou, N.S. Joshi, Engineered E. Coli Nissle 1917 for the delivery of matrix-tethered therapeutic domains to the gut, nature, Communications 10 (1) (2019) 5580.
[31] M.T. Cook, G. Tzortzis, D. Charalampopoulos, V.V. Khutoryanskiy, Microencapsulation of probiotics for gastrointestinal delivery, J. Control. Release 162 (1) (2012) 56–67.
[32] S. Razavi, S. Janfaza, N. Tasnim, D.L. Gibson, M. Hoorfar, Microencapsulating polymers for probiotics delivery systems: preparation, characterization, and applications, Food Hydrocoll. 120 (2021) 106882.
[33] Z.-J. Rong, H.-H. Cai, H. Wang, G.-H. Liu, Z.-W. Zhang, M. Chen, Y.-L. Huang, Ursolic acid ameliorates spinal cord injury in mice by regulating gut microbiota and metabolic, Changes 16 (2022).
[34] H.-Z. Zhu, Y.-D. Liang, Q.-Y. Ma, W.-Z. Hao, X.-J. Li, M.-S. Wu, L.-J. Deng, Y.-M. Li, J.-X. Chen, Xiaoyaosan improves depressive-like behavior in rats with chronic immobilization stress through modulation of the gut microbiota, Biomed. Pharmacother. 112 (2019) 108621.
[35] Q. Zhang, H. Yu, X. Xiao, L. Hu, F. Xin, X. Yu, Inulin-type fructan improves diabetic phenotype and gut microbiota profiles in rats, PeerJ 6 (2018) e4446.
[36] Y. Ma, Z. Tian, W. Zhai, Y. Qu, Insights on catalytic mechanism of CeO2 as multiple nanozymes, Nano Res. 15 (12) (2022) 10328–10342.
[37] V. Singh, S. Ahlawat, H. Mohan, S.S. Gill, K.A.-O.X. Sharma, Balancing reactive oxygen species generation by rebooting gut microbiota, (1365–2672 (Electronic)).

Trends in Food Science & Technology 142 (2023) 104227

Contents lists available at ScienceDirect

Trends in Food Science & Technology

journal homepage: www.elsevier.com/locate/tifs

Cytoprotection of probiotics by nanoencapsulation for advanced functions

Tong Zhang, Congdi Shang, Ting Du, Junchen Zhuo, Chen Wang, Bingzhi Li, Junnan Xu, Mingtao Fan, Jianlong Wang *, Wentao Zhang **

College of Food Science and Engineering, Northwest A&F University, Shaanxi, Yangling, 712100, China

ARTICLE INFO

Keywords:
Probiotics
Nanotechnology
Biological therapeutics
Molecular self-assembly
Biological membrane
Inflammatory bowel disease (IBD)

ABSTRACT

Background: Probiotics can enhance the health of the host by maintaining the balance of intestinal flora, but probiotic foods like yogurt have insufficient viable counts to reach prebiotic effects. To take advantage of probiotics, probiotics are fitted into sealed microcapsules in the size range of a few microns. Designing cytoprotective nanocoatings for probiotics is a promising strategy, as it addresses the limitations of microencapsulation including lack of particle size control, easy leak, and low in vivo efficiency.

Scope and approach: Probiotics by nanoencapsulation are based on the formation of nanocoating around individual probiotic cells, which can design specific nanocoating to protect probiotics and directly develop their advantages on the intestinal tract. Initially, this review delves into the issues for the application of probiotics and highlights the necessity of selecting cytoprotective nanocoating for probiotics. Furthermore, the method of major encapsulated probiotics utilizing nanocoating was introduced. Lastly, the challenges of nanocoating for probiotics are discussed.

Key findings and conclusions: Nanoencapsulation is a technique used to coat probiotics with nanomaterials, which enhances the bioavailability of drugs and expands their potential applications. The two main methods of encapsulating probiotics into nanocoating are biological and non-biological membranes. Despite some challenges in the production process (such as the security and complexity of the production process in further practical application), nano-coated probiotics are a promising approach for developing next-generation therapeutics that can be used for synergistic treatment and prevention.

1. Introduction

Probiotics, defined as live microorganisms and Generally Recognized as Safe (GRAS), confer many health benefits on the host when obtained sufficient amounts (Amiri, Rezaei Mokarram, Sowti Khiabani, Rezazadeh Bari, & Alizadeh Khaledabad, 2019; De Souza Oliveira, Perego, De Oliveira, & Converti, 2011; Michael, Phebus, & Schmidt, 2010). In recent years, there has been an increased interest in designing probiotic products due to their potential health benefits and disease prevention such as regulating host immune response, treating disease, maintaining gut homeostasis, producing bioactive substances, and enhancing gut barrier function (Lin, et al., 2021; Liu et al., 2022; Luo et al., 2022). Despite probiotics exhibiting excellent possibilities as microbial therapeutics and food supplements, they must be in a metabolically active state and present in sufficient amounts to be effective. Research has shown that viability of more than 10^6 CFU/g is needed to achieve biological benefits during delivery. (De Souza Oliveira, et al., 2011; Razavi, Janfaza, Tasnim, Gibson, & Hoorfar, 2021). Many challenges must be addressed for effective probiotics, including pH balance, oxygen levels, temperature, antimicrobial activity of bile salts, and competition from other bacteria. (Centurion, et al., 2021).

To solve these problems, microbial encapsulation strategies become promising methods for protecting probiotics during their oral delivery and storage time. Recently, microencapsulation has been one of the most common methods for increasing the probiotic survival rate under complex gastrointestinal conditions using hydrocolloid systems (Liu, et al., 2020; Sharma, Wasan, & Sharma, 2021; Yuan, Yin, Zhai, & Chen, 2022). Probiotics are fitted into sealed microcapsules in the size range of a few microns. These capsules, which are food-grade polymers mostly derived from polysaccharides, proteins, and lipids, degrade and release probiotics when exposed to specific conditions (Centurion, et al., 2021; Razavi et al., 2021). This method has exhibited significant advantages in

* Corresponding author.
** Corresponding author.
E-mail addresses: wanglong79@nwsuaf.edu.cn (J. Wang), zhangwt@nwsuaf.edu.cn (W. Zhang).

https://doi.org/10.1016/j.tifs.2023.104227
Received 18 August 2023; Received in revised form 27 October 2023; Accepted 28 October 2023
Available online 31 October 2023

improving probiotic viability but applied to practice still existing many problems including the control in particle size, leakage of probiotics, and low in *vivo* efficiency (Asgari, Pourjavadi, Licht, Boisen, & Ajalloueian, 2020; Iqbal et al., 2021; Trush et al., 2020).

Inspired by biofilms spontaneously produced by bacteria to survive in extreme conditions, which have the double advantage of resistance to environmental assaults and adhesion to particular positions, some researchers have tried to build biofilms on the surface of bacteria and design cytoprotective nanocoating for probiotics to markedly promote resistance and adherence in the gastrointestinal tract (GI) tract (Wang, et al., 2020). In contrast to microencapsulation methods based on probiotics into a micron-scale gel matrix, nanoencapsulation is based on the formation of nanocoating around individual probiotic cells, which can specifically design cytoprotective suit for the shortcomings of probiotics and directly adhere and proliferate on intestinal surfaces without requiring release from the encapsulating matrix (Anselmo, McHugh, Webster, Langer, & Jaklenec, 2016; Centurion et al., 2021).

Currently, the study of related probiotics-encapsulation is mainly focused on microbial encapsulation(Michael T. Cook, Tzortzis, Charalampopoulos, & Khutoryanskiy, 2012; Razavi et al., 2021). Nanoencapsulation for probiotics is rarely reported. Centurion et al. (2021) only overviewed the different probiotics encapsulation methods and nanoencapsulation strategies. This paper aims to introduce the importance of nanoencapsulation in delivery systems for probiotics to customize nanocoatings for probiotics according to requirements such as the protection of probiotics, improved adhesion, and superior therapeutic biological products. The framework diagram for this article is shown in Fig. 1. Table 1 shows the types and advantages of designing nanocoating for probiotics. The advantages of choosing cytoprotective nanocoating for probiotics were first described through literature examples (Fig. 2). Besides, the most important encapsulated strategies are first reviewed and their advantages for probiotics are highlighted (Figs. 3–4). Finally, the challenges of designing nanocoating for probiotics were discussed.

2. Dilemmas for application of probiotics

According to the World Health Organization (WHO) definition, probiotics are "live microorganisms conferring a health benefit on the host when administered in adequate amounts." Probiotics consumption has many beneficial effects, such as regulation of intestinal flora, production of antimicrobial, anticarcinogenic and substances, enhancing the body's immunity, relieving lactose intolerance, reducing serum cholesterol, and providing therapeutic benefits for intestinal diseases (Li, et al., 2019; Liu et al., 2022; Monteagudo-Mera, Rastall, Gibson, Charalampopoulos, & Chatzifragkou, 2019; Oak & Jha, 2019). The necessary condition for probiotics to work is a large amount of living probiotics to survive and colonize the mucosal membrane of the intestine, but this condition is difficult to achieve. Therefore, choosing the correct microbial encapsulation strategy is important for the application of probiotics. Dilemmas for the application of probiotics were as follows.

2.1. Complicated environment

It is generally known that, to exert health benefits, probiotics need to retain the viability and activity in the lower digestive tract, so these organisms should withstand adverse conditions such as gastric acid and bile in the upper gastrointestinal tract (GIT) to ensure survival rate (Ding & Shah, 2007; Farahmand et al., 2022). Thereinto, gastric acid may lead to cell death due to altered cell surface permeability by abundant H^+ in the stomach, and all bile can inhibit the growth of bacteria depending on its concentration, in which many Gram-positive probiotic organisms such as *Bifidobacterium* and *Lactobacillus* genera are restrained by bile acid, while Gram-negative organisms including *Escherichia coli* are not affected(Anselmo, et al., 2016; Ding & Shah, 2007). More importantly, most bowel diseases such as inflammatory bowel disease (IBD) can also seriously impede the growth of probiotics due to producing excessive reactive oxygen species (ROS) (Zhang et al., 2016; Zhu et al., 2022). ROS has a strong oxidation effect on lipids and proteins on the surface of probiotics, which can cause major damage to the cell wall of bacteria and lead to their inactivation (Liu et al., 2022; Singh, Ahlawat, Mohan, Gill, & Sharma, 2022; Yang et al., 2022).

Encapsulation has been used as an important tool to protect the probiotics and improve their survival due to the lower viability of probiotics used in fermented and other dairy products (How & Pui, 2021; Krasaekoopt, Bhandari, & Deeth, 2003; Zhao et al., 2019). Freeze-drying becomes an ideal choice for protecting encapsulated probiotic products to maintain a sufficient quantity of viable cells. The condition of commercially successful selected probiotic products is that they retain viability during product shelf-life when probiotics suffer freeze-drying with milled into a homogenous powder and encapsulated in the absence of oxygen and low water content (Wang, et al., 2019). To improve gastrointestinal function, it is recommended to consume probiotics at a daily intake of approximately 10^8 CFU/mL. However, the production of dried probiotics involves stressful procedures that can result in cell damage. Even with cryoprotectants, as few as 0.1% of cells survive, which is insufficient for daily requirements. (Her, Kim, & Lee, 2015). Production of probiotics keeping active is especially challenging

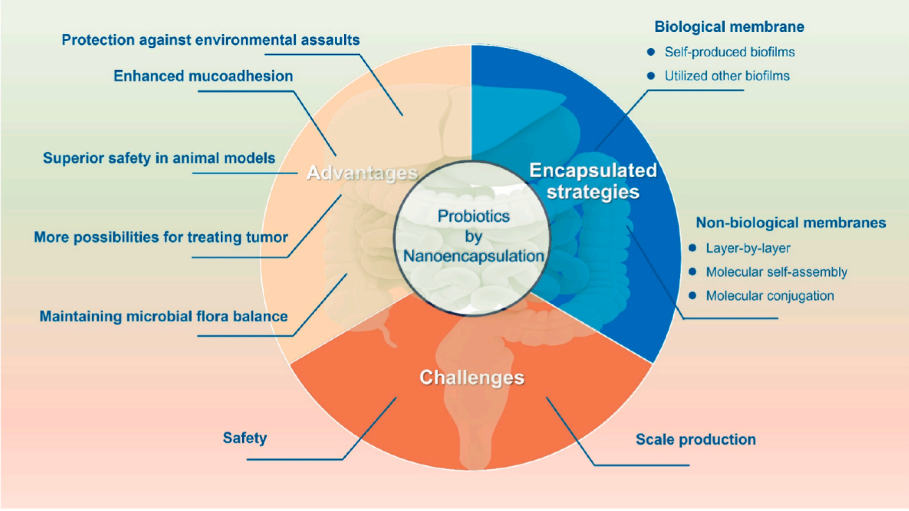

Fig. 1. The advantages, encapsulated strategies, and challenges of probiotics by nanoencapsulation.

Table 1
The types and advantages of designing nanocoating for probiotics.

Type		Materials	Probiotics	Advantages	Ref.
Biological membranes		self-produced biofilms	*Bacillus subtilis*	Superior resistance and adhesion capacity.	(X. Wang et al., 2020)
		Lipid membrane	*Escherichia coli* Nissle 1917	Significantly improved survival against various extreme conditions and enhanced oral efficacies in prevention and treatment	Z. Cao, Wang, et al. (2019)
		Erythrocyte membrane	*Escherichia coli Nissle* 1917	Low inflammatory response and improved colonization abilities in disease sites	Z. Cao, Cheng, et al. (2019)
		Yeast membrane with β-glucan	*Escherichia coli* Nissle 1917	Protected coated EcN from the insults of the gastrointestinal environments; the maintenance of microbiome composition protects the intestinal barrier from injury	Lin, et al. (2021)
		Spore coat	*Bacillus coagulans*	Resistance to extreme environments, anti-inflammatory properties, promotion of epithelial barrier recovery, natural affinity for probiotics, and restoration of gut barrier integrity	Song, et al. (2021)
Non-biological membranes	Layer-by-layer	Chitosan and alginate	*Bacillus coagulans*	Improved the survival of probiotics in oral delivery; unchanged morphology of coated probiotics	Anselmo, et al. (2016)
		2D CoCuMo-layered double hydroxides (LDH) nanosheets	*Lactobacillus acidophilus*	A tumor-microenvironment-responsive platform;	(Y. Yang et al., 2023)
		Silicene nanosheets	*Escherichia coli* Nissle 1917	Resisted gastric acid and treating colitis	Coqueiro, et al. (2019)
	Molecular conjugation	Avidin-biotin	*Lactobacillus casei, Escherichia coli*, and *Bacillus coagulans*	Improved colonization rate of probiotics and the ability to exclude pathogenic bacteria in *vitro*; the excellent adhesion of synthetic adhesins in gastrointestinal	Vargason, et al. (2020)
		β-cyclodextrin, adamantanic acid and dextran	*Clostridium butyricum*	Effectively enhanced the adhesion of probiotic and regulating intestinal flora	Zheng, et al. (2020)
		nano-enzyme and boronic acid–poly (ethylene glycol)	*Bifidobacterium longum*	Reduced inflammation caused by artificial enzymes; improved bacterial viability to rapidly reshape the intestinal barrier functions and restore the gut microbiota.	(F. Cao et al., 2023)
	Molecular self-assembly	Tannic acids (TA) and ferric ions (FeIII)	*Escherichia coli* Nissle1917	Enhanced resistance; avoided the negative effects of antibiotics in the gastrointestinal tract	Fan, et al. (2022)
		TA-Ca^{2+} and Mucin	*Escherichia coli* Nissle1917	superior resistance, strong adhesiveness, and distinctly down-regulate inflammation with ROS scavenging	(X. Yang et al., 2022)
		TA/Fe (III) MPN and enteric L100 layers	*Escherichia coli* Nissle1917	pH-responsive degradation; prolonged the retention time	(J. Liu et al., 2021)
		Polydopamine	*Lactobacillus helveticus* and *Lactobacillus plantarum*	enhanced the survival in gastric environment, and improvd capabilities of adhesion and scavenge oxygen radical	Centurion, et al. (2022)
		Polydopamine and hybrid immunoactive nanosurface	*Escherichia coli* Nissle1917	provoked innate immunity and suppressed tumor growth	(Y. Liu et al., 2023)
		Polydopamine and triple immune nanoactivators	*Escherichia coli* Nissle1917	The potent antitumor effects	(J. Li et al., 2022)
		Norepinephrine, poly (propylene sulfide) and hyaluronic acid	*Escherichia coli* Nissle1917	Having the ability of scavenge oxygen radicals; improving the viability at environmental assaults and mucoadhesive capability	(J. Liu et al., 2022)

due to both oxygen toxicity and damage during manufacture.

2.2. Lack of capabilities with mucoadhesion and colonization

The capabilities of mucoadhesion and colonization for probiotics are still difficult, which may limit the effect of oral probiotic supplements such as the regulation of intestinal flora (Fan, Wasuwanich, Rodriguez-Otero, & Furst, 2022). Probiotics were accelerated removal from the intestine due to constant peristalsis of the gastrointestinal tract. This physiological factor is responsible for the limited intestinal colonization of probiotics (Ajalloueian, et al., 2022; Giordani et al., 2018; Yang et al., 2022). Microencapsulation approaches, commonly used encapsulation for probiotics, have been applied to solve probiotic-specific delivery challenges (Chen, Meenu, & Xu, 2022; Xie et al., 2023). Although these methods have been successful in protecting probiotic cells against environmental assaults to enhance survival benefits in the GI tract due to preventing direct contact between probiotics and the environment (Michael T. Cook et al., 2012), these strategies significantly reduce adhesion and growth on intestinal surfaces, hindering probiotics from providing health benefits.

3. The advantages of designing cytoprotective nanocoating for probiotics

The development of a cytoprotective nanocoating for probiotics is based on the formation of nanofilms within individual cells using materials that can adhere and colonize surfaces, enabling probiotic cells to act directly on specific sites. Designing cytoprotective nanocoating for probiotics is a promising method for the protection of probiotics. Probiotics encapsulated in nanocoating can unlock a potential new model in oral delivery (Song, et al., 2019). We can tailor the nanocoating and increase the functional groups, thus improving the bioavailability of drugs and expanding the potential for probiotics by nanoencapsulation. The necessities and advantages of probiotics by customization nanocoating according to requirements are shown in this section.

3.1. Protection against environmental assaults

The problem of survival rate for probiotics during lyophilization can be effectively solved by customization nanocoating. Fan et al. (2022) designed a protected next-generation nanocoating (TA/Fe (III) MPN) for single probiotics during lyophilization, even in the absence of cryoprotectants. Because MPNs are structurally rigid, they may provide additional protection during lyophilization. Compared with the uncoated bacteria, *E. coli* 1917 exhibited higher viable counts, and the count of coated *E. coli* 1917 had a 3-fold increase in cryoprotectant-free phosphate citrate buffer (Fig. 2a). More importantly, the MPN-coated cells showed the fastest speed of growth after reconstitution, which highlighted the protective ability of nanocoating.

Another key limitation of the survival rate for probiotics is

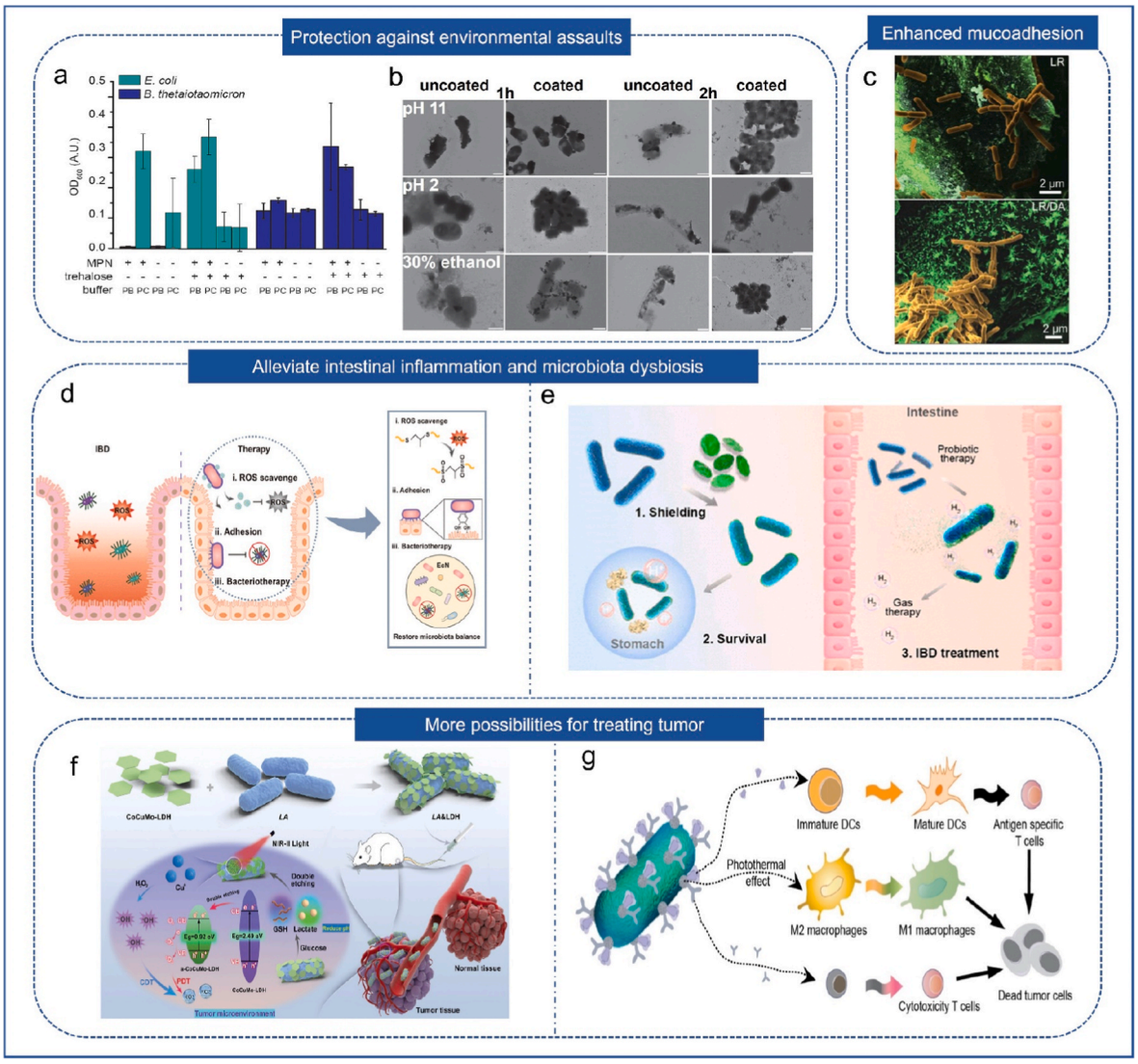

Fig. 2. (a) The growth of uncoated and coated probiotics in the presence and absence of MPNs and cryoprotectants (Fan, et al., 2022). Copyright © 2022, American Chemical Society. (b) TEM images of uncoated and coated probiotics at extreme environment (Z. Cao, Wang, et al., 2019). Copyright © 2019, Springer Nature. (c) SEM images of the adherence of uncoated and coated probiotics to Caco-2 cells (LR: uncoated probiotics; LR/DA: coated probiotics) (Centurion, et al., 2022). Copyright © 2022, Wiley-VCH GmbH. (d) Schematic illustration of nanocoating for probiotics with the features of scavenging ROS and regulating intestinal flora (J. Liu et al., 2022). Copyright © 2022, the American Association for the Advancement of Science's. (e) Schematic illustration of assembly and treatment for coated probiotics (Y.-X. Zhu et al., 2023). Copyright © 2023, American Chemical Society. (f) Schematic illustration of preparation of tumor-targeting platform using probiotics coated with nanosheets (Y. Yang et al., 2023). Copyright © 2023 Wiley-VCH GmbH. (g) Schematic illustration of tumor-specific antigens and checkpoint blocking antibodies decorated probiotics (J. Li et al., 2022). Copyright © 2022 Wiley-VCH GmbH.

environmental factors including acid accumulation and changes in the storage and transportation environment during the storage period (Li, et al., 2016). Harsh gastrointestinal (GI) conditions including low pH in the stomach and high concentration of bile salts in the small intestine are harmful to many probiotics in oral delivery (Dimitrellou et al., 2016). Nano-encapsulated probiotics form the nanocoating to isolate the complex environment and probiotics. Therefore, we also need to tackle key issues by improving the resistance of probiotics in harsh GI conditions via designing special nanocoating. The utilization of probiotics encapsulated in specialized nanocoating is anticipated to provide a novel solution for safeguarding these microorganisms against environmental stressors. Centurion et al. (2022) designed a self-encapsulating nanocoating using dopamine for probiotics which proved this nanocoating could help probiotics improve survival rate at the simulated gastric fluid. Cao, Wang, Pang, Cheng, and Liu (2019) demonstrated that probiotics encapsulated in nanocoating using lipid membrane via self-assembly could be improved resistance in an extreme environment. As is shown in Fig. 2b, coated probiotics, which were exposed to extreme environments (pH = 2 and 11, 30% ethanol), maintained the integrity of bacteria compared with uncoated probiotics, meanwhile, had a higher survival rate than uncoated probiotics in synthetic GI tract environments.

3.2. Enhanced mucoadhesion to oral delivery

Despite the need for specific protection within the stomach, delivered probiotics are anticipated to shed this protective layer prior to intestinal colonization to better perceive their surrounding microenvironment and interact with the indigenous microbiota therein (Zhu, et al., 2023). Therefore, the development of suitable materials for bacterial nano-coatings plays a crucial role in enhancing mucoadhesion for probiotics in oral delivery. Choosing the suitable nanocoating can consider the adhesion of materials in the intestinal mucus layer, e.g. mucin interacting with the intestinal mucus layer through hydrogen

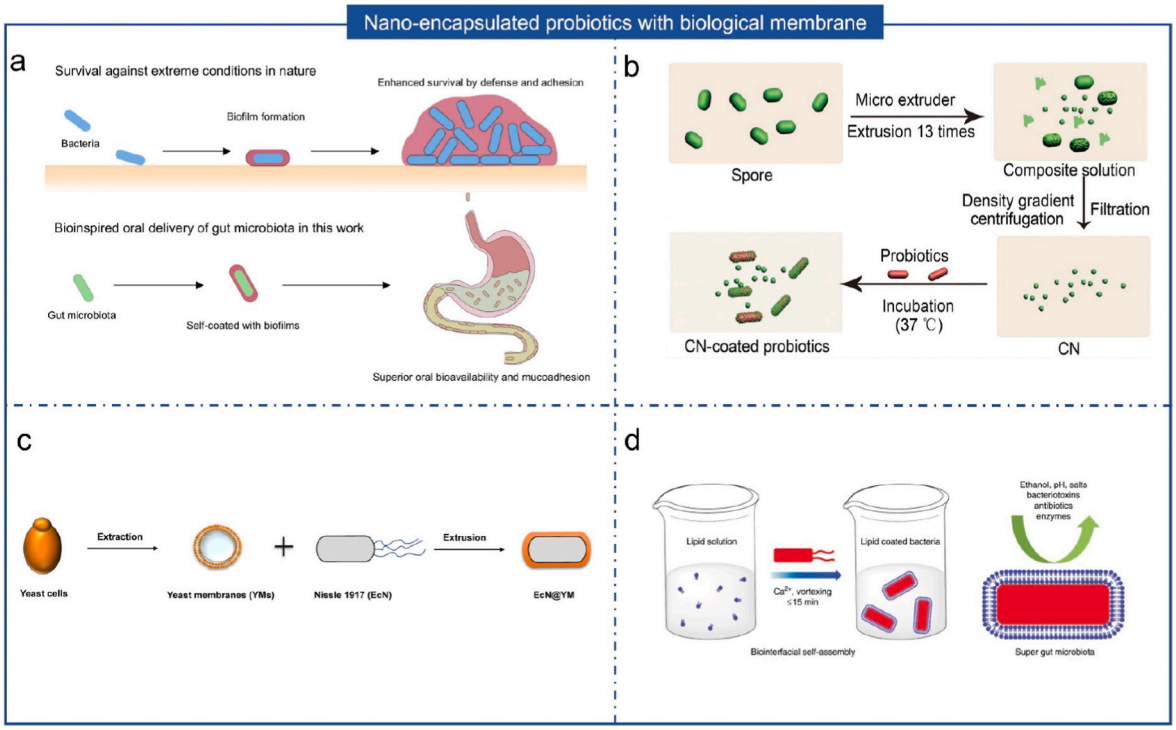

Fig. 3. (a) Schematic illustration of biofilm formation of bacteria in nature and bioinspired oral delivery of gut microbiota with self-coating with biofilms (X. Wang et al., 2020). Copyright © 2020, the American Association for the Advancement of Science's. (b) Schematic illustration of spore coat nanomaterial (CN)-coated probiotics (Song, et al., 2021). Copyright © 2021 Wiley-VCH GmbH. (c) Copyright © 2021, the American Association for the Advancement of Science's. (d) Schematic illustration of self-assembly of lipid membrane for probiotics (X. Wang et al., 2020). Copyright © 2019, Springer Nature.

bonding, disulfide bonding, and hydrophobic forces, polydopamine (PDA) of structures similar to mucin, and self-produced biofilm. X. Yang et al. (2022) developed a strategy for probiotics coated with mucin and tannic acid (TA) (EcN@TA-Ca2+@Mucin), which found that, for EcN@TA-Ca2+@Mucin, fluorescence signals in colon slices were present on days 3 and 6, whereas, other treatments only on days 3 detected fluorescence signals, indicating excellently intestinal adhesion of the mucin-coated probiotic system. As shown in Fig. 2c, the adhesion of probiotics with PDA-formed by phenolic polymerization to Caco-2 cells is higher than probiotics without PDA (Centurion, et al., 2022). Wang et al. (2020) showed a biofilm, acting as an adhesive and defending against external threats, for a single probiotic by self-coating, which indicated that compared with clinical *Bacillus subtilis* (BS) and individual biofilm-coated BS (BCBS), bacteria coated with biofilm fragments (FCBS) exhibited stronger adhesion whether in small intestine, large intestine or cecum, and also proved that coating with biofilms for probiotics was necessary to resist environmental threats in oral delivery, such as acidic stomach conditions, antibiotics and penetration of bile acids.

3.3. New ways to alleviate intestinal inflammation and microbiota dysbiosis

Gut microbiota composition plays many crucial roles in human health such as the synthesis of essential vitamins and prevention of pathogen invasion, but is susceptible to many environmental factors including an unbalanced diet, lack of physical activity, and smoking (Ke, et al., 2021; Rowland et al., 2018). The main health claims of probiotics are the regulation of microbiota composition and improvement in immune response, so probiotic supplementation is an important treatment in several diseases such as inflammatory bowel disease (IBD) (Coqueiro, Raizel, Bonvini, Tirapegui, & Rogero, 2019). Patients with IBD can present intestinal barrier alterations, which may lead to changes in microbiota and microbial metabolites, thus inducing subsequent immune cell activation and intestinal inflammation (Caruso, Lo, & Núñez, 2020). Microbial therapeutics are a promising prospect in maintaining gut homeostasis, and preserving barrier integrity (Wu & Wu, 2012).

In general, probiotics can be directly applied to treat diseases, but need to be through low pH in the stomach and harsh environment in the small intestine (e.g. the presence of bile salts) tract, ensuring that probiotics retain viability after reaching the desired site. Cao, Wang, et al. (2019) confirmed that the cytoprotection nanocoating by self-assembly of lipid membrane for probiotics had a good result in the prevention and treatment of IBD, which the major performances were that treating mice (coated-probiotic) significantly reduced the inflammation and weight loss. Besides protecting probiotics, probiotics by nanoencapsulation also can add nano-scale drugs to the surface of nanocoating for probiotics or utilize nano-scale drugs to form nanocoating, which is a new way to treat and prevent intestinal disease at a cellular level. The overproduction of reactive oxygen species (ROS) and inflammatory factors, and disturbance in the bacterial microbiota are the major causes of intestinal inflammation (Cao, et al., 2023; Zhou et al., 2022). To solve this problem, nanocoating with additional functions is born to treat IBD. Designed a nanocoating for probiotics with the features of scavenging ROS and regulating intestinal flora, selecting a hydrophobic polymer with scavenging ROS ability to covalent binding with the self-assembly poly-norepinephrine on the probiotic surface (Fig. 2d). This delivery system can effectively scavenge ROS, improve the delivery of probiotics, and maintain microbiota homeostasis (Liu, et al., 2022). Lin et al. (2021) utilized **yeast membrane (YM)** embedded β-glucan to camouflage living probiotics to facilitate phagocytosis of microfold cells (M cells) distributed in the intestinal epithelium, thus, efficacious enhancing strong mucosal immune responses, proving that coated-probiotics could help mice recover alteration of intestinal flora and maintain intestinal health, and effectively reduce the bacterial infection-induced intestinal barrier impairment. As shown in Fig. 2e, this work developed a delivery system for probiotic/gas dual-mode therapy to treat IBD by utilizing

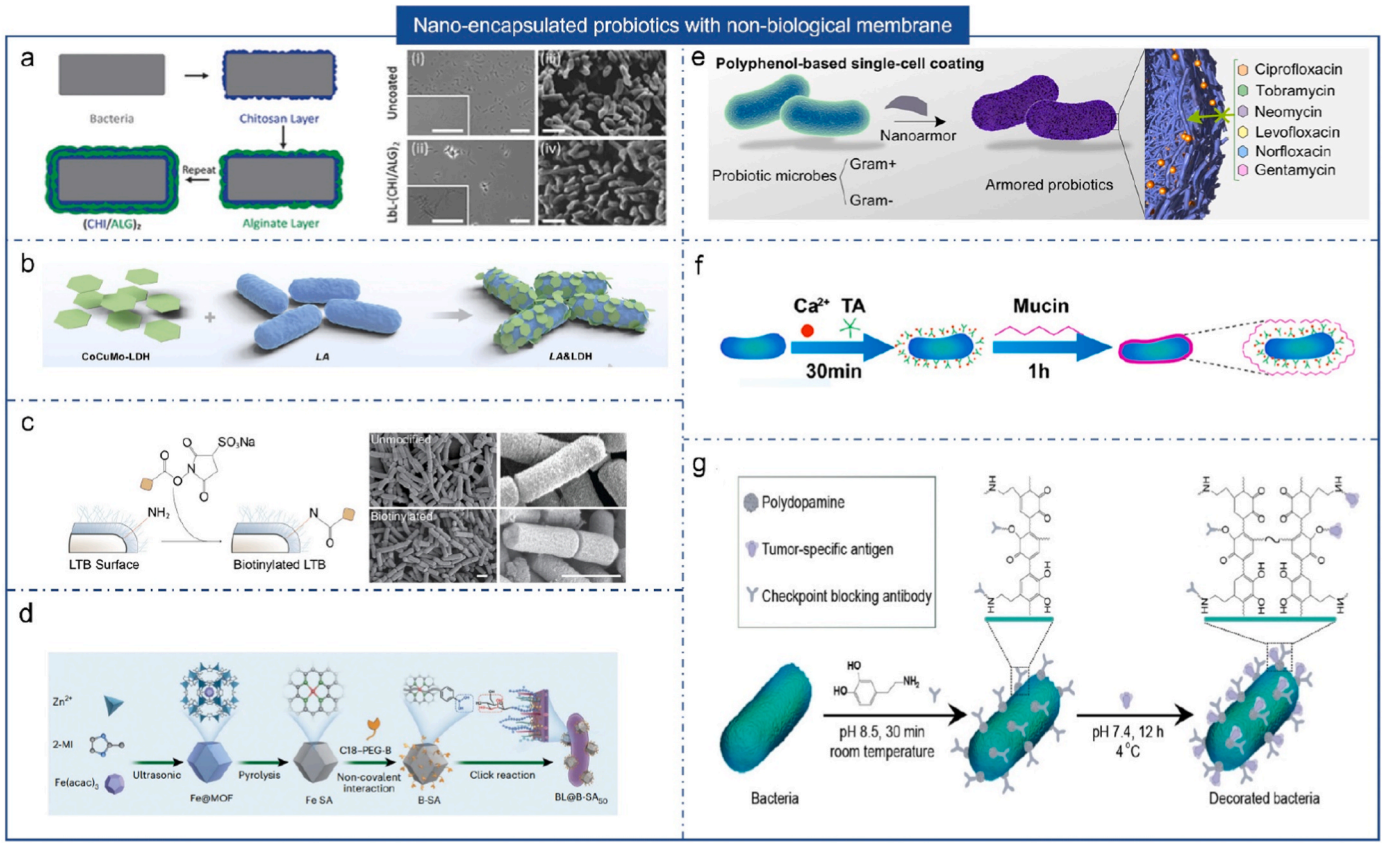

Fig. 4. Schematic illustration of nanocoating for (a) probiotic at their surface by using the alternately deposition of chitosan and alginate (Anselmo, et al., 2016), Copyright © 2016 Wiley-VCH GmbH, (b)probiotics combined the 2D CoCuMo layered-double-hydroxide (LDH) nanosheets (Y. Yang et al., 2023), Copyright © 2023 Wiley-VCH GmbH, (c) biotin and streptavidin to conjugate the surface of probiotic (Vargason, et al., 2020), Copyright © 2020 Wiley-VCH GmbH, (d) linker of boronic acid–poly (ethylene glycol) to bind probiotics and artificial-enzymes (F. Cao et al., 2023), Copyright © 2023 Springer Nature, (e) TA and Fe (III) ions protected probiotics, Copyright © 2022 Springer Nature, (f) tannic acid and mucin (X. Yang et al., 2022), Copyright © 2022 Springer Nature, (g) a triple immune nanoactivators anchored at the surface of polydopamine to protect probiotics (J. Li et al., 2022). Copyright © 2022 Wiley-VCH GmbH.

covalently hydrogen-terminated silicene nanosheets (SiH NSs) were leveraged to *E. coli Nissle* 1917 (EcN), which showed that EcN@SiH exhibited the better therapeutic effect for IBD. Therefore, SiH NSs could release hydrogen amplifying the therapeutic efficacy of probiotic treatment in a synergistic manner (Zhu, et al., 2023).

3.4. More possibilities for disease prevention

Probiotics capable of modulating gastrointestinal function through oral delivery offer superior biocompatibility, and can be served as a disease prevention platform. Currently, the studies of nano-encapsulated probiotics are mainly focused on cancer treatment and prevention, but the application of nano-encapsulated probiotics in nutrition and health improvement is rarely reported. Probiotics such as *C. butyricum* and *Akkermansia muciniphila* can ferment polysaccharides to produce anti-inflammatory short-chain fatty acids (SCFA). Among them, *C. butyricum* is found to be widely distributed in tumor tissues and selected for targeting colon tumors (Dalile, Van Oudenhove, Vervliet, & Verbeke, 2019; Zheng et al., 2020). To help probiotics target colon tumors, prebiotics, which can improve intestinal adhesion, and promote the fermentation of probiotics to produce a large amount of anti-cancer SCFA, are used at the surface of probiotics. It has been demonstrated that *C. butyricum* was encapsulated in prebiotics to exhibit excellent tumor-targeting capacity and tumor suppression rate (Zheng, et al., 2020). Targeted and therapeutic oncology drugs can load on the surface of probiotics by designing nanocoating. Song et al. (2019) showed an autonomous self-assembled nanoparticles (NPs) generator for probiotics, which coloaded the therapeutic drugs to the NPs reaching the effect of synergistic treatment. This therapeutic strategy exhibited satisfactory anti-inflammatory and tumor suppression effects and helped restore the gut barrier integrity and maintain the balance of intestinal flora. Because the tumor microenvironment (TME)-induced nanosheets can boost its photodynamic activity for singlet oxygen generation under 1270 nm laser irradiation. As shown in Fig. 2f, it developed a tumor-targeting platform for TME-responsive photosensitizers, which used probiotics coated with nanosheets and effectively achieved tumor eradication and prolonged the life of mice through photodynamic therapy under 1270 nm laser irradiation. To decrease the inflammatory reaction, bodily clearance, and side effects, the camouflaged probiotics using erythrocyte membranes had been designed by the low immunogenicity and anti-phagocytic nature of erythrocyte membranes, which not only remained inherent bioactivities probiotics, it also improved colonization abilities in disease sites (Cao, Cheng, Wang, Pang, & Liu, 2019). To improve cancer immunotherapy, tumor-specific antigens and checkpoint-blocking antibodies are attached to the bacterial surface, resulting in multimodal and long-acting therapeutics that significantly inhibit tumor growth and extend the survival of mice (Fig. 2g).

Inspired by treating tumors for probiotics, rational designing the surface of probiotics can be applied in nutrition and health improvement. Using cell-mediated biointerfacial assembly, we can refer to this model and combine the active substance, including natural active materials, effective ingredients for health care, and therapeutic drugs, into the surface of probiotics, which can increase the functions of probiotics and create more possibilities for disease prevention and the development of new health products.

3.5. Superior safety in animal models

Safety is the primary consideration in designing nanocoatings. At present, there are no security issues observed in animal models and cell experiments by rational designing nanocoating. Liu et al. (2021) designed biomaterial coating for probiotics, in mice models, which showed the superior efficacy of treatment and no significant side effects in *vivo*. Cao et al. (2023) exhibited that excellent therapeutic effects were demonstrated in canine models in addition to the mouse model.

4. The methods for designing the nanocoating for probiotics

Previous studies, mimicking the sporulation process, showed that a protective and degradable shell formed in yeast cells could lead to enhanced cellular tolerance against external stressors (Park, et al., 2014). Wang et al. (2020) utilized the capacity of self-formed biofilms of bacteria to shield probiotics, resulting in superior resistance and adhesion capabilities for the protected probiotics. Designing nanocoating that is based on the formation of nanofilms around individual probiotic cells can provide many advantages such as improving vivo resistance, adhesion, and even illness-preventing power. In this section, we will discuss how to design a nanocoating for probiotics. This process can be divided into two main parts: biological and non-biological membranes. We will also explore the benefits and drawbacks of various nanocoating methods for probiotics. It's worth noting that these methods have been used for different living cells, but their applications for probiotic encapsulation are not in vogue and require further exploration.

4.1. Biological membrane

Encapsulation in the biological membrane has been reported in two approaches at present including self-produced biofilms of probiotics (Wang, et al., 2020) and utilized other biofilms (Cao, Cheng, et al., 2019). Encapsulation using self-produced biofilms can retain a long-lasting protective effect for probiotics due to forming self-produced biofilms during bacterial growth. The limitations of this approach are that most probiotics don't possess the ability to produce biofilms. Wang et al. (2020) reported that *Bacillus subtilis*, secreting abundant exopolysaccharides and proteins, enabled the trigger of the formation of a self-produced biofilm in appropriate culture conditions, demonstrating superior resistance and adhesion capacity (Fig. 3a).

Other biofilms such as erythrocyte membranes (Cao, Cheng, et al., 2019), spore coats (Song, et al., 2021), yeast membranes (Lin, et al., 2021), and thin lipid membranes via supramolecular assembly (Cao, Wang, et al., 2019) also could be designed as the nanocoating. Among them, encapsulation in extruding erythrocyte membrane can successfully camouflage probiotics due to their low immunogenicity and long circulation properties, thereby exhibiting many advantages including the low inflammatory response, reduced elimination by macrophage, and almost unchanged viabilities (Cao, Cheng, et al., 2019). Because spore coats of probiotics had many benefits including high tolerance, superior anti-inflammatory effect, and excellent biocompatibility, Wang et al. (2020) made spore coats become multi-functional coat nanoparticles by mechanical force extrusion, encapsulating single probiotic cells (Fig. 3b), and encapsulated probiotics maintained the integrity of spore coat components and formed the functional armor exhibiting excellent protection, bioactivity, and colonization ability. Probiotics are camouflaged inside yeast membrane-embedded β-glucan, ensuring living bacteria into lymphoid follicles and enhancing mucosal immune responses (Fig. 3c). Results of staining could demonstrate yeast wall (blue) binding to probiotics (red) and the nano-coating was further confirmed in transmission electron microscopy (TEM) (Lin, et al., 2021). Thin lipid membrane via supramolecular assembly with dioleoylphosphatydic acid, cholesterol, and calcium phosphate buffer could coat probiotics by vortexing with biocompatible lipids (Fig. 3d), which significantly improved survival rate in various against environmental assaults and enhanced oral efficacies in prevention and treatment.

To summarize, utilizing biological membranes as nanocoating presents numerous benefits such as reduced inflammatory response and natural affinity for probiotics (Cao, Cheng, et al., 2019; Song et al., 2021). Therefore, encapsulating probiotics within biological membranes significantly enhances their resistance to harsh environments, promotes colonization and proliferation, and maintains intestinal homeostasis, meanwhile, has not changed the viability and bioactivity of probiotics, but the complicated extraction and production process needs to be overcome in the future.

4.2. Non-biological membrane

Besides biological membrane, non-biological membrane was widely used in making nanocoating for probiotics, which is based on chemical methods to modify the surface of probiotics and encapsulate probiotics. The coatings prevent direct contact of bacteria with the environment to improve viability and stability in acid and enzyme insults but also decrease adhesion in the intestinal mucosa. Therefore, designing a group that enhances adhesion to modify bacteria becomes the main purpose. For example, primary amino groups on bacterial surfaces were converted to free thiols using in-situ chemical reactions, demonstrating that modified bacteria achieved excellent attachment in mucin-enriched jejunum (Luo, et al., 2022). Currently, many methods have been applied in designing nanocoating for probiotics including layer-by-layer, molecular conjugation, molecular self-assembly, and choosing suitable methods according to present needs to tune surface functions for probiotics.

4.2.1. Layer-by-layer

Layer-by-layer (LbL) encapsulation, known as LbL self-assembly, utilizes the intermolecular forces, including electrostatic forces, host-guest interactions, hydrogen bonds, etc., of two or more materials to deposit them alternately on the template surface (An, Huang, & Shi, 2018; Qiu, Song, & Fan, 2015; Qiu, Song & Fan, 2015, 2015). Among them, electrostatic force, which utilizes electrostatic interaction between the polyanions and polycations, is the most commonly used intermolecular force for LBL self-assembly (Qin, Wang, Tang, & Guo, 2010; Yan, Deng, & Wang, 2007; Chenghui Zhang, Li, Aliakbarlu, Cui, & Lin, 2022). Although electrostatic LbL strategies have been applied to multiple substrates such as living cell, planar, and colloidal substrates, their application for probiotic cells is still rarely used, which the main reasons are that this method is time-consuming and the complexity of the sedimentary process makes it difficult to scale up (Centurion, et al., 2021).

At present, some researchers have produced a nanofilm for probiotics at their surface by using the alternate deposition of chitosan (cationic polysaccharide) and alginate (anionic polymer) (Fig. 4a), thereby realizing single-cell encapsulation and protecting probiotic against environmental assaults (Anselmo, et al., 2016; Cook, Tzortzis, Khutoryanskiy, & Charalampopoulos, 2013). Among them, Cook et al. (2013) first characterized the material properties in *vitro* testing, which demonstrated that this formulation improved the survival of probiotics and targeted probiotics cells to the intestine. Then, Anselmo et al. (2016) proved that the morphology of coated probiotics was not significantly changed because of their smooth nanoscale features, and the delayed cell division of coated probiotics by using alternately polymer deposition had been discovered. This strategy improved the viability of probiotics in oral delivery but still reinforced intestinal adhesion.

The utilization of 2D inorganic nanosheets as nanocoating for probiotics has become a prevailing trend, due to their multifaceted properties including high specific surface area, ultrathin microstructure, fascinating physiochemical properties, and desirable biocompatibility and biodegradability (You, Yang, Zhang, Lin, & Shi, 2021). The thinness of these nanosheets can respond rapidly to external signals such as light, which leads to utility in a variety of optical therapies, including imaging

applications, photothermal therapy, and photodynamic therapy (Chimene, Alge, & Gaharwar, 2015). Yang et al. (2023) effectively combined the 2D CoCuMo layered-double-hydroxide (LDH) nanosheets and *Lactobacillus acidophilus* via electrostatic interaction, which makes the probiotics become tumor-microenvironment-responsive platform due to the feature of photodynamic therapy for nanosheets (Fig. 4b). In other studies, copolymer-modified two-dimensional H-silicene nanosheets electrostatically, which could generate an anti-inflammatory gas (hydrogen) in response to the neutral/weakly alkaline environment, coated with probiotics to resist gastric acid and treat colitis (Zhu, et al., 2023).

4.2.2. Molecular conjugation

Molecular conjugation refers to linking two partners from small molecules to large and sometimes functionally complex biopolymers (Schreiber & Smith, 2019). In designing nano-suit, molecular conjugation encapsulation is a common surface functionalization method by adding a biological coupling agent to connect biomaterials and single probiotics, which usually used connection types are avidin-biotin interactions, host-guest assembly and click reaction (Cao, et al., 2023; Vargason, Santhosh, & Anselmo, 2020; Zheng et al., 2020).

The avidin-biotin technology, one of the strongest non-covalent interactions, is known for the ability to rapidly film forming with a surface either non-biological surfaces or most biological membranes (Gao, Sun, Li, & He, 2022; Henry et al., 2018; Chenzhen Zhang, He, Vedadghavami, & Bajpayee, 2020). Vargason et al. (2020) utilized the strong and specific interaction between biotin and streptavidin by using a biological coupling agent (sulfo-N-hydroxysuccinimide, sulfoNHS) and biocompatible ester-amine chemistry to conjugate the surface of probiotics, which had improved the colonization rate of probiotics and the ability to exclude pathogenic bacteria in *vitro* due to the excellent adhesion of synthetic adhesins in gastrointestinal (GI), and did not affect the bacterial viability and maintained metabolic activity during surface-modification process (Fig. 4c). However, the defect could lead to the development of antibiotic resistance and alteration of intestinal flora due to requiring antibiotics to achieve the colonization of probiotics.

Supramolecular self-assemblies play an important role in biomedical and biotechnology fields through host-guest interactions due to their potential applications such as the photoswitched biointerfaces utilizing host–guest interactions realizing the capture and release of control cells (Liu, Shi, & Ma, 2019; Sinawang, Osaki, Takashima, Yamaguchi, & Harada, 2020). The strategy of using prebiotics (dextran) encapsulated single probiotic, effectively enhancing the adhesion of probiotics and regulating intestinal flora, via host-guest interactions between β-cyclodextrin and adamantanic acid has been reported (Zheng, et al., 2020). However, the structure of the coated biointerface in a single probiotic may cause uneven phenomena due to the probabilistic connection between dextran and adamantanic acid.

The click reaction is a facile and high-yield method to bind two molecular building blocks together under mild water-tolerant conditions, with minimal by-products. (Deng, Shavandi, Okoro, & Nie, 2021; Liang & Astruc, 2011). Inspired by the fast and facile boronic acid vicinal-diol-based click reaction. Boronic acids with alcohols lead to the high stability of boronate esters formation, allowing to building of reversible molecular assemblies (Gómez-Jaimes & Barba, 2014). Cao et al. (2023) chose the linker of boronic acid–poly (ethylene glycol) to bind *Bifidobacterium longum* and artificial enzymes (Fig. 4d). This study relied on the ROS-scavenging ability of artificial enzymes and the advantage of probiotics helping the targeting and retention of artificial enzymes to reshape a healthy immune system in IBD (Cao, et al., 2023).

4.2.3. Molecular self-assembly

Self-assembly can be defined that the molecular components spontaneously arrange themselves into ordered hierarchical structures by specific intermolecular interactions, which can form biological nanostructures such as the construction of cell membranes and the coating of biomacromolecules (Dong, Wang, He, She, & Dong, 2020; Yadav, Sharma, & Kumar, 2020). Protective coatings for probiotics also have been applied to form biological nanostructures by molecular self-assembly. Phenolic compounds play a pivotal role in daily life due to their attractive biological properties containing antioxidant, antibacterial, anti-inflammatory, the ability of radical scavenging pigmentation, and flavoring of plants and food products (Du, Li, et al., 2023; Kang et al., 2023). In the most recent decade, the feature of “green” and low-cost polyphenols has become desirably engineering of biologically functional materials (Du, Wang, et al., 2023; Rahim et al., 2018). Phenolic compounds with excellent adherence usually can be used to construct thin films on diverse substrates which have two methods including metal–phenolic networks (MPN) assembly and oxidative self-polymerization assembly (Fichman & Schneider, 2021; Liang et al., 2018; Rahim et al., 2018; Md Arifur Rahim, Kristufek, Pan, Richardson, & Caruso, 2019; Zhong et al., 2018). At present, MPN and oxidative self-polymerization assembly have been applied to form the nanocoating. Tannin (TA) and dopamine (DA) are the two main materials used in the design of nanocoating.

The coordination of metal-phenolic complexes has become an increasingly popular synthetic strategy for surface engineering. In particular, the combination of catechol and transition metal ions with synthetic materials has been an important subject in biomimetic functional materials. For designing nanocoating, a notable example is a coordination-driven assembly of MPN for surface film formation of probiotics such as TA and Fe (III) ions (Centurion, et al., 2021; Md Arifur Rahim et al., 2019). Fan et al. (2022) reported the formation of a rigid barrier for probiotics by using three polyphenols and Fe (III) ions and found that the formative barrier of TA had the best effect, and MPN successfully enhanced resistance to adversity for probiotics. Another research exhibited the formation of nano armor (TA and Fe (III) ions) protected bacteria from the action of antibiotics (Fig. 4e), on the surface, and effectively absorbed the antibiotics reducing antibiotic-associated diarrhea in combination therapy of antibiotics and probiotics, avoiding the negative effects of antibiotics in the gastrointestinal tract (Pan, et al., 2022). To achieve increasing diversity, many researchers have attempted to add a new layer on the surface of MPN. Because probiotics colonized and grew in the mucus layer, Yang et al. (2022) developed a strategy probiotic coated with tannic acid and mucin (EcN@TA--Ca^{2+}@Mucin), which exhibited superior resistance, strong adhesiveness, and distinctly down-regulate inflammation with ROS scavenging (Fig. 4f). Another double-layer coating strategy encapsulates probiotics in a TA/Fe (III) MPN (interior layer) and enteric L100 layers (Liu, et al., 2021). This strategy could take advantage of pH-responsive degradation of enteric L100 protecting probiotics against the acidic environment in the stomach to selectively release TA-probiotics and prolong the retention time of probiotics in the intestine due to the strong mucoadhesive of TA after L100 disassociation.

Oxidative self-polymerization assembly bearing catechol groups have become frequent surface engineering strategies. The catalytic systems using redox-active transition metals are known to activate phenolic oxidation and induce crosslinking reactions accelerating self-polymerization assembly. The catechol-containing compounds including dopamine (DA), caffeic acid, and pyrocatechol have been investigated for the cell-mediated ability of probiotics to trigger the oxidative self-polymerization (Centurion, et al., 2022; Md Arifur Rahim et al., 2019). Polydopamine, a mussel-inspired polymer produced by marine organisms, has many properties including strength, toughness, and durability (Mrówczyński, 2018). Under a cytocompatible condition, diverse cells simply co-deposit with dopamine, including bacteria, fungi, and mammalian cells. The results showed that, compared with uncoated bacteria, decorated cells show higher bioavailability in the gut and higher accumulation in the inflamed tissue (Pan, et al., 2021). Centurion et al. (2022) reported that the capability of phenolic self-assembly, DA turned into PDA, was harnessed to form a multifunctional nanocoating on the individual probiotic surface with the accumulation of Mn ion by

probiotics, displaying the predominant cytoprotective to enhance the survival in the gastric environment, and improving capabilities of adhesion and scavenge oxygen radicals. To achieve the goal of eliciting dual anticancer and antiviral immunity, the hybrid immunoreactive nanosurface is linked to polydopamine nanoparticles, which could be coated with bacteria to further provoke innate immunity and suppress tumor growth (Liu, et al., 2023). A triple immune nanoactivator was also anchored at the surface of polydopamine, which further proved the potent antitumor effects (Li, et al., 2022). These studies provided more possibilities for the preparation of multimodal and long-acting therapies for cancer immunotherapy (Fig. 4g). Norepinephrine (NE), belonging to the catecholamine group, was also applied to encapsulate individual probiotics by oxidative self-polymerization assembly. In their nanocoating, the outer layer loaded nanoparticles having the ability to scavenge oxygen radicals (Liu, et al., 2022).

5. The challenges of designing nanocoating for probiotics

Although research papers have been published on the design of nanocoating for probiotics, this method has yet to be applied in reality for two reasons. On the one hand, the synthesis methods of nanocoating have the possibility of difficulty in scale production. For example, biological membranes were used as nanocoatings, which would confront the problem of a complex extraction process. LbL assembly method fabricated nanocoating was faced with the problem of time-consuming and complex steps, thus generating difficulty to scale up. To realize surface functions for probiotics, some study has added organic synthesis in designing nanocoatings such as the formation of nanoparticles of poly (propylene sulfide) and hyaluronic acid, which will face many problems including complex operation and cumbersome separation process. Therefore, the development of simple and multifunctional nanocoating plays an important role in broadening the application for nano-coated probiotics. On the other hand, clinical trials in nano-encapsulated probiotics have not been reported. Although the application of nanocoating in animal and cell models exhibits a satisfactory therapeutic effect and no damage to the body, the lack of clinical trials and safety evaluations prevents the practical application of nanocoating for probiotics. Therefore, the research of nanocoating for probiotics is still in its infancy, and application in practice remains to require further exploration and effort.

6. Conclusion and outlook

Designing nanocoating to modulate the properties of probiotics is a promising method to increase the possibility of the delivery system. We overview the importance of cytoprotective nano-armor for probiotics in delivery systems and how to customize these nano-armor. The encapsulation process of probiotics via designing nanocoating was presented here, which exhibits many benefits including disease prevention, the balance of intestinal flora, enhanced resistance in harsh conditions, and the adhesion of the intestinal tract. Furthermore, we can tailor the nanocoating of probiotics to meet specific requirements, achieving a synergistic treatment effect. Lastly, the review covers the primary techniques and challenges for nano-encapsulated probiotics has been reviewed.

Although this work discusses various methods for designing nanocoatings, the process of creating nanocoatings for probiotics is still in its early stages. The ideal combination of nanocoating and probiotics should involve mild reaction conditions, convenient operations, and no harm to the bacterial cell. Customized nanocoating according to different requirements still considers mutual biocompatibility. Meanwhile, the connection between the bacterial cell wall and nanocoating plays an important role in maintaining the activity of probiotics, so the problem of balance between the optimum formation condition of nanocoating and probiotic viability needs to be addressed. Additionally, we propose to explore plentiful biocompatible materials to become nanocoating for probiotics, which screening conditions for materials include coating capacity, toxicity, compatibility of coating conditions with living cells, adhesion performance, cost-effectiveness, ease of manipulation, and low inflammatory response. At present, there have been few reports of the nutrition and health improvement for nano-encapsulated probiotics in the food field, but with the advances in nanocoating of synthetic tools and based on promising probiotic properties for customizing nanocoating for probiotics, we are looking forward to further applying in the practice of nano-encapsulated probiotics.

Author contributions

Tong Zhang: Conceptualization, Investigation, Writing-original draft. **Congdi Shang**: Modification, Visualization. **Ting Du**: Modification, Visualization. **Junchen Zhuo**: Modification. **Chen Wang**: Visualization. **Bingzhi Li**: Visualization. **Junnan Xu**: Visualization. **Mingtao Fan**: Modification, Visualization. **Jianlong Wang**: Supervision, Writing-review & editing. Wentao Zhang: Resources, Writing-review & editing, Project administration.

Declaration of competing interest

The authors declare no competing interests.

Data availability

No data was used for the research described in the article.

Acknowledgments

This work was supported by the National Natural Science Foundation of China (31901794, 21675127, 22102133), the National Postdoctoral Program for Innovative Talents (BX20180263), the Young Talent Fund of University Association for Science and Technology in Shaanxi, China (2019-02-03), the Tang Scholar by Cyrus Tang Foundation and the Key Research and Development Program of Shaanxi Province (2022NY-001).

References

Ajalloueian, F., Guerra, P. R., Bahl, M. I., Torp, A. M., Te Hwu, E., Licht, T. R., et al. (2022). Multi-layer PLGA-pullulan-PLGA electrospun nanofibers for probiotic delivery. *Food Hydrocolloids, 123*, Article 107112.

Amiri, S., Rezaei Mokarram, R., Sowti Khiabani, M., Rezazadeh Bari, M., & Alizadeh Khaledabad, M. (2019). Exopolysaccharides production by Lactobacillus acidophilus LA5 and Bifidobacterium animalis subsp. lactis BB12: Optimization of fermentation variables and characterization of structure and bioactivities. *International Journal of Biological Macromolecules, 123*, 752–765.

An, Q., Huang, T., & Shi, F. (2018). Covalent layer-by-layer films: Chemistry, design, and multidisciplinary applications (vol 47, pg 5061, 2018). *Chemical Society Reviews, 47*, 5529-5529.

Anselmo, A. C., McHugh, K. J., Webster, J., Langer, R., & Jaklenec, A. (2016). Layer-by-Layer encapsulation of probiotics for delivery to the microbiome. *Advanced Materials, 28*, 9486–9490.

Asgari, S., Pourjavadi, A., Licht, T. R., Boisen, A., & Ajalloueian, F. (2020). Polymeric carriers for enhanced delivery of probiotics. *Advanced Drug Delivery Reviews, 161–162*, 1–21.

Cao, Z., Cheng, S., Wang, X., Pang, Y., & Liu, J. (2019a). Camouflaging bacteria by wrapping with cell membranes. *Nature Communications, 10*, 3452.

Cao, F., Jin, L., Gao, Y., Ding, Y., Wen, H., Qian, Z., et al. (2023). Artificial-enzymes-armed Bifidobacterium longum probiotics for alleviating intestinal inflammation and microbiota dysbiosis. *Nature Nanotechnology, 18*, 617–627.

Cao, Z., Wang, X., Pang, Y., Cheng, S., & Liu, J. (2019b). Biointerfacial self-assembly generates lipid membrane coated bacteria for enhanced oral delivery and treatment. *Nature Communications, 10*, 5783.

Caruso, R., Lo, B. C., & Núñez, G. (2020). Host–microbiota interactions in inflammatory bowel disease. *Nature Reviews Immunology, 20*, 411–426.

Centurion, F., Basit, A. W., Liu, J., Gaisford, S., Rahim, M. A., & Kalantar-Zadeh, K. (2021). Nanoencapsulation for probiotic delivery. *ACS Nano, 15*, 18653–18660.

Centurion, F., Merhebi, S., Baharfar, M., Abbasi, R., Zhang, C., Mousavi, M., et al. (2022). Cell-mediated biointerfacial phenolic assembly for probiotic nano encapsulation. *Advanced Functional Materials, 32*, Article 2200775.

Chen, Y. N., Meenu, M., & Xu, B. J. (2022). A narrative review on microencapsulation of obligate anaerobe probiotics Bifidobacterium, Akkermansia muciniphila, and faecalibacterium prausnitzii. *Food Reviews International, 38*, 373–402.

Chimene, D., Alge, D. L., & Gaharwar, A. K. (2015). Two-dimensional nanomaterials for biomedical applications: Emerging trends and future prospects. *Advanced Materials, 27*, 7261–7284.
Cook, M. T., Tzortzis, G., Charalampopoulos, D., & Khutoryanskiy, V. V. (2012). Microencapsulation of probiotics for gastrointestinal delivery. *Journal of Controlled Release, 162*, 56–67.
Cook, M. T., Tzortzis, G., Khutoryanskiy, V. V., & Charalampopoulos, D. (2013). Layer-by-layer coating of alginate matrices with chitosan-alginate for the improved survival and targeted delivery of probiotic bacteria after oral administration. *Journal of Materials Chemistry B, 1*, 52–60.
Coqueiro, A. Y., Raizel, R., Bonvini, A., Tirapegui, J., & Rogero, M. M. (2019). Probiotics for inflammatory bowel diseases: A promising adjuvant treatment. *International Journal of Food Sciences & Nutrition, 70*, 20–29.
Dalile, B., Van Oudenhove, L., Vervliet, B., & Verbeke, K. (2019). The role of short-chain fatty acids in microbiota–gut–brain communication. *Nature Reviews Gastroenterology & Hepatology, 16*, 461–478.
De Souza Oliveira, R. P., Perego, P., De Oliveira, M. N., & Converti, A. (2011). Effect of inulin as a prebiotic to improve growth and counts of a probiotic cocktail in fermented skim milk. *LWT - Food Science and Technology, 44*, 520–523.
Deng, Y. L., Shavandi, A., Okoro, O. V., & Nie, L. (2021). Alginate modification via click chemistry for biomedical applications. *Carbohydrate Polymers, 270*, Article 118360.
Ding, W. K., & Shah, N. P. (2007). Acid, bile, and heat tolerance of free and microencapsulated probiotic bacteria. *Journal of Food Science, 72*, M446–M450.
Dong, X. C., Wang, M., He, Q., She, A. Q., & Dong, Y. H. (2020). Atomistic liquid crystalline structures of discotic bent-core-like mesogens formed by hydrogen bonding and interchain interactions. *Journal of Molecular Modeling, 26*, 308.
Du, T., Li, X., Wang, S., Su, Z., sun, H., Wang, J., et al. (2023a). Phytochemicals-based edible coating for photodynamic preservation of fresh-cut apples. *Food Research International, 163*, Article 112293.
Du, T., Wang, S., Feng, J., Shen, Y., Wang, J., & Zhang, W. (2023b). Dual-mechanism tuned engineered polyphenols with cascade photocatalytic self-fenton reaction for sustainable biocidal coatings. *Nano Letters, 23*, 9563–9570.
Fan, G., Wasuwanich, P., Rodriguez-Otero, M. R., & Furst, A. L. (2022). Protection of anaerobic microbes from processing stressors using metal–phenolic networks. *Journal of the American Chemical Society, 144*, 2438–2443.
Farahmand, A., Ghorani, B., Emadzadeh, B., Sarabi-Jamab, M., Emadzadeh, M., Modiri, A., et al. (2022). Millifluidic-assisted ionic gelation technique for encapsulation of probiotics in double-layered polysaccharide structure. *Food Research International, 160*.
Fichman, G., & Schneider, J. P. (2021). Dopamine self-polymerization as a simple and powerful tool to modulate the viscoelastic mechanical properties of peptide-based gels. *Molecules, 26*, 1363.
Gao, F., Sun, H. Y., Li, X., & He, P. N. (2022). Leveraging avidin-biotin interaction to quantify permeability property of microvessels-on-a-chip networks. *American Journal of Physiology - Heart and Circulatory Physiology, 322*, H71–H86.
Giordani, B., Melgoza, L. M., Parolin, C., Foschi, C., Marangoni, A., Abruzzo, A., et al. (2018). Vaginal Bifidobacterium breve for preventing urogenital infections: Development of delayed release mucoadhesive oral tablets. *International Journal of Pharmaceutics, 550*, 455–462.
Gómez-Jaimes, G., & Barba, V. (2014). Boronate esters: Synthesis, characterization and molecular base receptor analysis. *Journal of Molecular Structure, 1075*, 594–598.
Henry, S., Williams, E., Barr, K., Korchagina, E., Tuzikov, A., Ilyushina, N., et al. (2018). Rapid one-step biotinylation of biological and non-biological surfaces. *Scientific Reports, 8*, 2845.
Her, J.-Y., Kim, M. S., & Lee, K.-G. (2015). Preparation of probiotic powder by the spray freeze-drying method. *Journal of Food Engineering, 150*, 70–74.
How, Y., & Pui, L. (2021). Effect of prebiotics encapsulated with probiotics on encapsulation efficiency, microbead size, and survivability: A review. *Journal of Food Measurement and Characterization, 15*, 4899–4916.
Iqbal, R., Liaqat, A., Chughtai, M. F. J., Tanweer, S., Tehseen, S., Ahsan, S., et al. (2021). Microencapsulation: A pragmatic approach towards delivery of probiotics in gut. *Journal of Microencapsulation, 38*, 437–458.
Kang, Y., Li, M., Han, Y., Sun, H., Dan, J., Liang, Y., et al. (2023). Tannic acid-derived selective capture of bacteria from apple juice. *Food Chemistry, 412*, Article 135539.
Ke, S. Z., Yu, Y. L., Xu, Q. L., Zhang, B., Wang, S. J., Jin, W. H., et al. (2021). Composition-activity relationships of polysaccharides from saccharina japonica in regulating gut microbiota in short-term high-fat diet-fed mice. *Journal of Agricultural and Food Chemistry, 69*, 11121–11130.
Krasaekoopt, W., Bhandari, B., & Deeth, H. (2003). Evaluation of encapsulation techniques of probiotics for yoghurt. *International Dairy Journal, 13*, 3–13.
Liang, L., & Astruc, D. (2011). The copper(I)-catalyzed alkyne-azide cycloaddition (CuAAC) "click" reaction and its applications. An overview. *Coordination Chemistry Reviews, 255*, 2933–2945.
Liang, H. S., Zhou, B., Li, J., Liu, X. N., Deng, Z. Y., & Li, B. (2018). Engineering multifunctional coatings on nanoparticles based on oxidative coupling assembly of polyphenols for stimuli-responsive drug delivery. *Journal of Agricultural and Food Chemistry, 66*, 6897–6905.
Li, Y., Liu, T., Zhang, X., Zhao, M., Zhang, H., & Feng, F. (2019). Lactobacillus plantarum helps to suppress body weight gain, improve serum lipid profile and ameliorate low-grade inflammation in mice administered with glycerol monolaurate. *Journal of Functional Foods, 53*, 54–61.
Li, S., Ma, C., Gong, G., Liu, Z., Chang, C., & Xu, Z. (2016). The impact of onion juice on milk fermentation by Lactobacillus acidophilus. *LWT - Food Science and Technology, 65*, 543–548.
Lin, S., Mukherjee, S., Li, J., Hou, W., Pan, C., & Liu, J. (2021). Mucosal immunity–mediated modulation of the gut microbiome by oral delivery of probiotics into Peyer's patches. *Science Advances, 7*, Article eabf0677.
Liu, Y., Liu, B., Li, D., Hu, Y., Zhao, L., Zhang, M., et al. (2020). Improved gastric acid resistance and adhesive colonization of probiotics by mucoadhesive and intestinal targeted konjac glucomannan microspheres. *Advanced Functional Materials, 30*, Article 2001157.
Liu, J., Li, W., Wang, Y., Ding, Y., Lee, A., & Hu, Q. (2021). Biomaterials coating for on-demand bacteria delivery: Selective release, adhesion, and detachment. *Nano Today, 41*, Article 101291.
Liu, Y. M., Shi, K. J., & Ma, D. (2019). Water-soluble pillar[n]arene mediated supramolecular self-assembly: Multi-dimensional morphology controlled by host size. *Chemistry–An Asian Journal, 14*, 307–312.
Liu, J., Wang, Y., Heelan, W. J., Chen, Y., Li, Z., & Hu, Q. (2022). Mucoadhesive probiotic backpacks with ROS nanoscavengers enhance the bacteriotherapy for inflammatory bowel diseases. *Science Advances, 8*, Article eabp8798.
Liu, Y., Zhang, M., Wang, X., Yang, F., Cao, Z., Wang, L., et al. (2023). Dressing bacteria with a hybrid immunoactive nanosurface to elicit dual anticancer and antiviral immunity. *Advanced Materials, 35*, Article 2210949.
Li, J., Xia, Q., Guo, H., Fu, Z., Liu, Y., Lin, S., et al. (2022). Decorating bacteria with triple immune nanoactivators generates tumor-resident living immunotherapeutics. *Angewandte Chemie, 134*, Article e202202409.
Luo, H., Chen, Y., Kuang, X., Wang, X., Yang, F., Cao, Z., et al. (2022a). Chemical reaction-mediated covalent localization of bacteria. *Nature Communications, 13*, 7808.
Luo, Y., De Souza, C., Ramachandran, M., Wang, S., Yi, H., Ma, Z., et al. (2022b). Precise oral delivery systems for probiotics: A review. *Journal of Controlled Release, 352*, 371–384.
Michael, M., Phebus, R. K., & Schmidt, K. A. (2010). Impact of a plant extract on the viability of Lactobacillus delbrueckii ssp. bulgaricus and Streptococcus thermophilus in nonfat yogurt. *International Dairy Journal, 20*, 665–672.
Monteagudo-Mera, A., Rastall, R. A., Gibson, G. R., Charalampopoulos, D., & Chatzifragkou, A. (2019). Adhesion mechanisms mediated by probiotics and prebiotics and their potential impact on human health. *Applied Microbiology and Biotechnology, 103*, 6463–6472.
Mrówczyński, R. (2018). Polydopamine-based multifunctional (Nano)materials for cancer therapy. *ACS Applied Materials & Interfaces, 10*, 7541–7561.
Oak, S. J., & Jha, R. (2019). The effects of probiotics in lactose intolerance: A systematic review. *Critical Reviews in Food Science and Nutrition, 59*, 1675–1683.
Pan, J., Gong, G., Wang, Q., Shang, J., He, Y., Catania, C., et al. (2022). A single-cell nanocoating of probiotics for enhanced amelioration of antibiotic-associated diarrhea. *Nature Communications, 13*, 2117.
Pan, C., Li, J., Hou, W., Lin, S., Wang, L., Pang, Y., et al. (2021). Polymerization-mediated multifunctionalization of living cells for enhanced cell-based therapy. *Advanced Materials, 33*, Article 2007379.
Park, J. H., Kim, K., Lee, J., Choi, J. Y., Hong, D., Yang, S. H., et al. (2014). A cytoprotective and degradable metal–polyphenol nanoshell for single-cell encapsulation. *Angewandte Chemie International Edition, 53*, 12420–12425.
Qin, Y. J., Wang, Y. Y., Tang, M. X., & Guo, Z. X. (2010). Layer-by-layer electrostatic self-assembly of anionic and cationic carbon nanotubes. *Chinese Chemical Letters, 21*, 876–879.
Qiu, T., Song, J., & Fan, L. J. (2015b). Preparation of fluorescent microspheres via layer-by-layer self-assembly. *Journal of Controlled Release, 213*, E103–E104.
Qiu, T., Song, J., Fan, L.-J., & J. J. o. c. r. o. j. o. t. C. R. S. (2015a). Preparation of fluorescent microspheres via layer-by-layer self-assembly. *Journal of Controlled Release, 213*, e103–e104.
Rahim, M. A., Bjornmalm, M., Bertleff-Zieschang, N., Ju, Y., Mettu, S., Leeming, M. G., et al. (2018). Multiligand metal-phenolic assembly from green tea infusions. *ACS Applied Materials & Interfaces, 10*, 7632–7639.
Rahim, M. A., Kristufek, S. L., Pan, S., Richardson, J. J., & Caruso, F. (2019). Phenolic building blocks for the assembly of functional materials. *Angewandte Chemie International Edition, 58*, 1904–1927.
Razavi, S., Janfaza, S., Tasnim, N., Gibson, D. L., & Hoorfar, M. (2021). Microencapsulating polymers for probiotics delivery systems: Preparation, characterization, and applications. *Food Hydrocolloids, 120*, Article 106882.
Rowland, I., Gibson, G., Heinken, A., Scott, K., Swann, J., Thiele, I., et al. (2018). Gut microbiota functions: Metabolism of nutrients and other food components. *European Journal of Nutrition, 57*, 1–24.
Schreiber, C. L., & Smith, B. D. (2019). Molecular conjugation using non-covalent click chemistry. *Nature Reviews Chemistry, 3*, 393–400.
Sharma, M., Wasan, A., & Sharma, R. K. (2021). Recent developments in probiotics: An emphasis on Bifidobacterium. *Food Bioscience, 41*, Article 100993.
Sinawang, G., Osaki, M., Takashima, Y., Yamaguchi, H., & Harada, A. (2020). Supramolecular self-healing materials from non-covalent cross-linking host-guest interactions. *Chemical Communications, 56*, 4381–4395.
Singh, V., Ahlawat, S., Mohan, H., Gill, S. S., & Sharma, K. K. (2022). Balancing reactive oxygen species generation by rebooting gut microbiota. *Journal of Applied Microbiology, 132*, 4112–4129.
Song, Q., Zhao, H., Zheng, C., Wang, K., Gao, H., Feng, Q., et al. (2021). A bioinspired versatile spore coat nanomaterial for oral probiotics delivery. *Advanced Functional Materials, 31*, Article 2104994.
Song, Q., Zheng, C., Jia, J., Zhao, H., Feng, Q., Zhang, H., et al. (2019). A probiotic spore-based oral autonomous nanoparticles generator for cancer therapy. *Advanced Materials, 31*, Article 1903793.

Trush, E. A., Poluektova, E. A., Beniashvilli, A. G., Shifrin, O. S., Poluektov, Y. M., & Ivashkin, V. T. (2020). The evolution of human probiotics: Challenges and prospects. *Probiotics and Antimicrobial Proteins, 12*, 1291–1299.

Vargason, A. M., Santhosh, S., & Anselmo, A. C. (2020). Surface modifications for improved delivery and function of therapeutic bacteria. *Small, 16*, Article 2001705.

Wang, X., Cao, Z., Zhang, M., Meng, L., Ming, Z., & Liu, J. (2020). Bioinspired oral delivery of gut microbiota by self-coating with biofilms. *Science Advances, 6*, Article eabb1952.

Wang, C. N., Wang, M., Wang, H., Sun, X. M., Guo, M. R., & Hou, J. C. (2019). Effects of polymerized whey protein on survivability of Lactobacillus acidophilus LA-5 during freeze-drying. *Food Science and Nutrition, 7*, 2708–2715.

Wu, H.-J., & Wu, E. (2012). The role of gut microbiota in immune homeostasis and autoimmunity. *Gut Microbes, 3*, 4–14.

Xie, A. J., Zhao, S. S., Liu, Z. F., Yue, X. Q., Shao, J. H., Li, M. H., et al. (2023). Polysaccharides, proteins, and their complex as microencapsulation carriers for delivery of probiotics: A review on carrier types and encapsulation techniques. *International Journal of Biological Macromolecules, 242*.

Yadav, S., Sharma, A. K., & Kumar, P. (2020). Nanoscale self-assembly for therapeutic delivery. *Frontiers in Bioengineering and Biotechnology, 8*, 127.

Yan, X. J., Deng, Y. H., & Wang, X. G. (2007). pH Effect on electrostatic layer-by-layer self-assembly of a side-crain azo polyelectrolyte. *Acta Polymerica Sinica*, 440–445.

Yang, Y., Hu, T., Bian, Y., Meng, F., Yu, S., Li, H., et al. (2023). Coupling probiotics with 2D CoCuMo-LDH nanosheets as a tumor-microenvironment-responsive platform for precise NIR-II photodynamic therapy. *Advanced Materials*, Article 2211205. n/a.

Yang, X., Yang, J., Ye, Z., Zhang, G., Nie, W., Cheng, H., et al. (2022). Physiologically inspired mucin coated Escherichia coli Nissle 1917 enhances biotherapy by regulating the pathological microenvironment to improve intestinal colonization. *ACS Nano, 16*, 4041–4058.

You, Y., Yang, C., Zhang, X., Lin, H., & Shi, J. (2021). Emerging two-dimensional silicene nanosheets for biomedical applications. *Materials Today Nano, 16*, Article 100132.

Yuan, Y. K., Yin, M., Zhai, Q. X., & Chen, M. S. (2022). The encapsulation strategy to improve the survival of probiotics for food application: From rough multicellular to single-cell surface engineering and microbial mediation. *Critical Reviews in Food Science and Nutrition*, 1–17.

Zhang, C., He, T., Vedadghavami, A., & Bajpayee, A. G. (2020). Avidin-biotin technology to synthesize multi-arm nano-construct for drug delivery. *MethodsX, 7*, 100882-100882.

Zhang, C., Li, C., Aliakbarlu, J., Cui, H., & Lin, L. (2022). Typical application of electrostatic layer-by-layer self-assembly technology in food safety assurance. *Trends in Food Science & Technology, 129*, 88–97.

Zhang, Q., Tao, H., Lin, Y., Hu, Y., An, H., Zhang, D., et al. (2016). A superoxide dismutase/catalase mimetic nanomedicine for targeted therapy of inflammatory bowel disease. *Biomaterials, 105*, 206–221.

Zhao, W. B., Liu, Y. H., Latta, M., Ma, W. T., Wu, Z. R., & Chen, P. (2019). Probiotics database: A potential source of fermented foods. *International Journal of Food Properties, 22*, 197–216.

Zheng, D.-W., Li, R.-Q., An, J.-X., Xie, T.-Q., Han, Z.-Y., Xu, R., et al. (2020). Prebiotics-encapsulated probiotic spores regulate gut microbiota and suppress colon cancer. *Advanced Materials, 32*, Article 2004529.

Zhong, Q. Z., Pan, S. J., Rahim, M. A., Yun, G., Li, J. H., Ju, Y., et al. (2018). Spray assembly of metal-phenolic networks: Formation, growth, and applications. *ACS Applied Materials & Interfaces, 10*, 33721–33729.

Zhou, J., Li, M., Chen, Q., Li, X., Chen, L., Dong, Z., et al. (2022). Programmable probiotics modulate inflammation and gut microbiota for inflammatory bowel disease treatment after effective oral delivery. *Nature Communications, 13*, 3432.

Zhu, Y., Wang, Q. H., Chen, Y., Xie, Y. T., Han, G. H., Liu, S., et al. (2022). Living probiotics-loaded hydrogel microspheres with gastric acid resistance and ROS triggered release for potential therapy of inflammatory bowel disease. *ACS Applied Polymer Materials, 5*, 957–967.

Zhu, Y.-X., You, Y., Chen, Z., Xu, D., Yue, W., Ma, X., et al. (2023). Inorganic nanosheet-shielded probiotics: A self-adaptable oral delivery system for intestinal disease treatment. *Nano Letters, 23*, 4683–4692.